



UNIVERSITY OF BOLOGNA
DEPARTMENT OF PHYSICS AND ASTRONOMY
MASTER DEGREE IN SCIENCE OF CLIMATE

~ · ~

ACADEMIC YEAR 2024–2025

CLIMATE SYSTEM MODELING NOTES

Prof.
Antonio Navarra

Author
Students of the Course

Last updated: December 13, 2024
[Latest version](#)

The contents of these notes stem from the course of Climate System Modeling taught by Prof. **Antonio Navarra**¹ at University of Bologna for the academic year 2024/2025 and from his notes available at wanderer.cmcc.it². The main textbook used to teach this course is Washington and Parkinson (2005).

The source code is available on [Github](#).

¹[CMCC, Unibo](#)

²If prompted, use the credentials: { user: cmcc , psw: pD8phJg3e76J }

Contents

1 Physical description of the climate system	5
1.1 Atmosphere	5
1.1.1 Atmospheric composition	5
1.1.2 The Vertical Temperature Profile	5
1.1.3 Regional and Seasonal Variations	7
1.1.4 The equilibrium energy balance	7
1.1.5 The General Circulation of the Atmosphere	8
1.1.6 The time averaged zonal general circulation	10
1.1.7 The horizontal general circulation & wind	11
1.1.8 Mean Sea Level Pressure and The Sea Surface Temperature	11
1.1.9 Energy balances in the atmosphere	12
1.2 Oceans	12
1.2.1 Oceanic Composition	13
1.2.2 Thermal structure	13
1.2.3 The salinity structure of the ocean	14
1.2.4 Influence of the ocean	17
1.2.5 Ocean currents	17
1.3 Ice	20
1.4 Interconnections between atmosphere, ocean and ice	23
1.4.1 Atmosphere effect	23
1.4.2 Ocean effect	23
1.4.3 Ice	25
2 Fundamental equations and processes	27
2.1 Background	27
2.1.1 The Earth spherical coordinates system	27
2.1.2 Rates of change of fluid properties over time: Eulerian vs Lagrangian description	27
2.2 Primitive equations	29
2.2.1 Momentum equation	29
2.2.2 Mass conservation	30
2.2.3 First law of thermodynamics	31
2.2.4 Hydrostatic balance	32
2.2.5 Geostrophic balance	33
2.2.6 The full set of governing equations for the atmosphere	34
2.2.7 β -plane approximation	35
2.3 Linear solutions to the primitive equations	35
2.3.1 Waves	36
2.4 Homogeneous flows	37
2.4.1 The vorticity equation on the β -plane	39
2.5 Rossby waves	40
2.6 Fundamental processes	41

2.6.1	Radiation	41
2.6.2	Moisture	46
2.6.3	Clouds	47
2.6.4	Surface Processes	48
2.6.5	Hydrology	49
A	Mathematical Complements	51
A.1	Vector calculus	51
A.1.1	Gradient	51
A.1.2	Divergence	51
A.1.3	Curl	52
A.2	Spherical harmonics	52
A.2.1	Mathematical Definition of Spherical Harmonics	52
A.2.2	Spherical Harmonics Expansion of Functions on the Sphere	53
A.2.3	Properties of Spherical Harmonics	54
A.2.4	Applications of Spherical Harmonics in Climate Models	54
A.3	EOF: Empirical Orthogonal Functions	55
A.3.1	Eigenvalue decomposition → Singular Value Decomposition	56
A.3.2	Limitations	57
A.3.3	Variance	57
A.3.4	Covariance	57
A.3.5	Correlation	57
A.4	Space-time splittings	58
A.4.1	Zonal means	58
A.4.2	Time means	58
A.4.3	Higher order quantities	58
	Bibliography	61

Chapter 1

Physical description of the climate system

Last updated: 2024-12-02 23.47

Source file: [chapter-intro.tex](#)

1.1 Atmosphere

1.1.1 Atmospheric composition

The atmosphere is a gaseous envelope that surrounds the Earth, acting as a protective envelope essential for life. It is composed of a mechanical mixture of several gases, with *nitrogen* (N_2) being the most abundant (78 % of the volume of dry air), followed by *oxygen* (O_2) 20.95 %, *argon* (Ar) 0.93 %, and *carbon dioxide* CO_2 0.037 %. Trace gases like *Neon* (Ne), *helium* (He), *methane* (CH_4), and *hydrogen* (H) also contribute to its composition, along with varying amounts of water vapor, which depend on factors such as location, evaporation rates, and temperature.

This gaseous mixture is held to the Earth by gravity, which causes the atmosphere to exert a pressure. Near the surface, the pressure is greatest, approximately 1.013×10^3 mbar at sea level, and it decreases with altitude. This reduction in pressure reflects the compressibility of gases, making the atmosphere densest near the ground. This characteristic distinguishes the atmosphere from the ocean, where the density remains relatively uniform due to the near incompressibility of liquids.

1.1.2 The Vertical Temperature Profile

The atmosphere exhibits a distinct temperature profile that changes with altitude and varies depending on the region and season. These variations define the layers of the atmosphere, each with unique characteristics and processes.

- **The Troposphere:** is the lowest layer, extending from the surface up to about 17 kilometers in the tropics and 8 km to 9 km in polar regions.
- In this layer, the temperature generally decreases with altitude at an average rate of $6.4^\circ C km^{-1}$. This gradient arises because the surface absorbs heat from the sun and transfers it to the air above, while higher altitudes are farther from this heat source. The troposphere is also the region where most weather phenomena, including clouds and storms, occur, making it the most dynamic part of the atmosphere.

At the upper boundary of the troposphere, known as the **tropopause**, the temperature reaches its minimum and remains constant for a short distance. In tropical regions, the

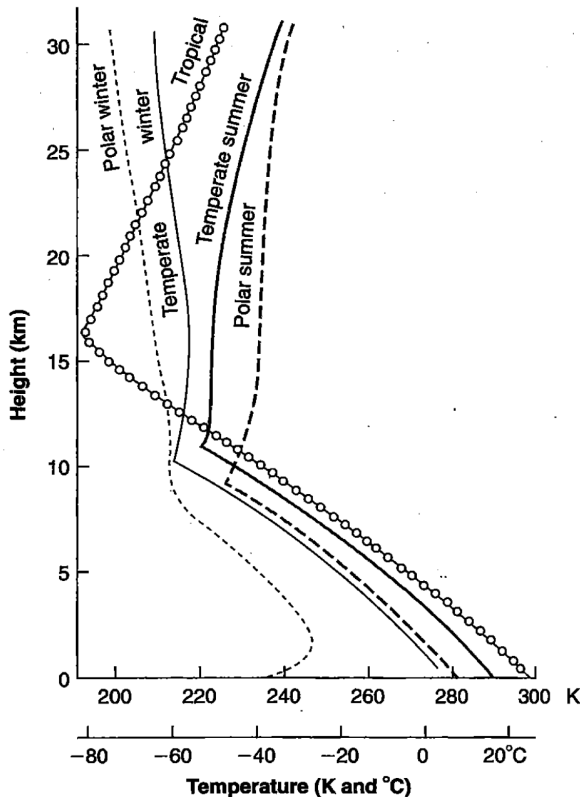


Figure 1.1: Atmospheric temperature profiles for different regions and seasons. Climatological average from Dobson (1968).

tropopause is particularly cold, with temperatures dropping to about 190 K, marking one of the coldest points in the Earth's atmosphere.

- **The Stratosphere:** Above the tropopause lies the stratosphere, a more stable layer where temperatures either remain constant or begin to rise with altitude. This increase is primarily due to the absorption of ultraviolet radiation by ozone molecules, which warms this part of the atmosphere. Unlike the troposphere, the stratosphere lacks the turbulence and weather systems associated with surface heating.
- **The Thermosphere:** the temperature continues to increase steadily with altitude. This layer is less influenced by surface-level processes and is instead heated by the absorption of high-energy solar radiation, making it the hottest layer of the atmosphere.

	Troposphere (sum/win)	Tropopause	Stratosphere
poles	280 K / 235 K	9 km: 230 K / inversion (1.5 km/2 km)	Slow Warming / Slow Cooling
midlat	290 K / 280 K	10 km: 220 K	Slow Warming / Slow Cooling
tropics	300 K	17 km: 190 K	Warming

Table 1.1: Temperature characteristics (expressed in K) in different atmospheric layers.

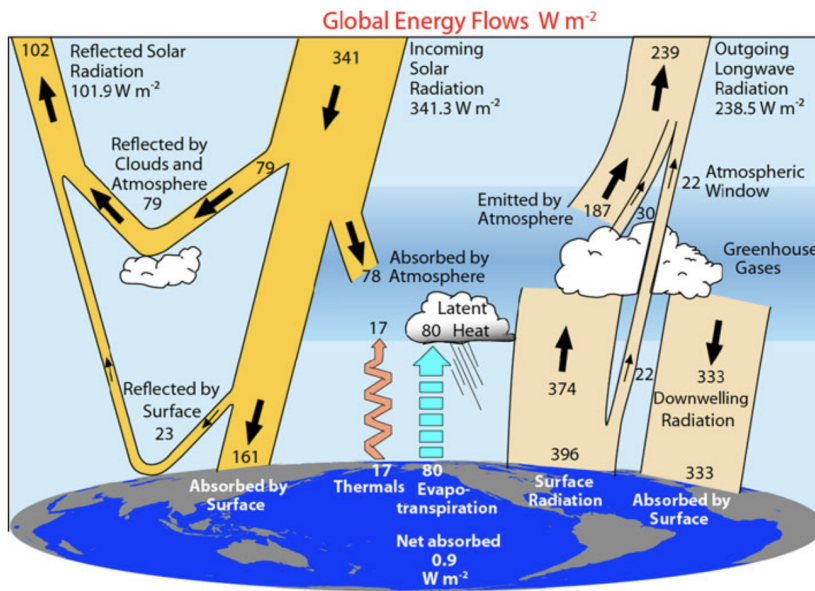


Figure 1.2: The mean global annual Earth's energy budget for 2000–2005 (W m^{-2}). The broad arrows indicate the schematic flow of energy in proportion to their importance. Taken from Trenberth and Fasullo (2012).

1.1.3 Regional and Seasonal Variations

As one can grasp from Figure 1.1 and from Table 1.1, temperature profiles in the atmosphere are not uniform and vary significantly between regions and seasons.

- **Polar regions:** In summer, temperatures near the surface reach about 280 K, decreasing gradually with height. In winter, surface temperatures can plummet to 235 K, but a slight increase often occurs at altitudes of 1.5–2 due to a phenomenon called *temperature inversion*. This inversion, caused by the cooling of surface air, reverses the usual trend of decreasing temperature with height.
- **Tropical regions:** Surface temperatures remain relatively constant, averaging around 300 K. However, as altitude increases, the temperature drops sharply, reaching the coldest point at the tropopause (about 190 K).
- **Mid-latitudes:** The temperature profile combines characteristics of both polar and tropical regions, varying more noticeably between seasons.

1.1.4 The equilibrium energy balance

The vertical temperature gradient in the atmosphere is maintained by complex energy processes, including the absorption and radiation of heat, convection, and interactions with the Earth's surface. These processes vary with latitude and season, creating the dynamic and layered structure of the atmosphere.

Inversions, which occur when surface air cools significantly, disrupt the usual temperature gradient, particularly in the troposphere. These events highlight the intricate balance of energy transfer within the atmosphere and its impact on weather and climate.

All the energy that enters the Earth's climate system comes from the sun. A portion of this solar energy is absorbed in the Earth's climate system and must be balanced with outgoing energy to maintain the observed overall equilibrium state of the climate. Such outgoing energy is emitted by the Earth's surface, the oceans, the atmosphere, the ice, and all of its life forms.

The Earth's climate system is driven by a balance between incoming solar radiation and outgoing terrestrial radiation, as illustrated in Figure 1.2. Of the 341.3 W m^{-2} of solar radiation reaching the Earth, approximately 23 W m^{-2} is reflected by the surface, 79 W m^{-2} is reflected by clouds and the atmosphere, and the remaining 161 W m^{-2} is absorbed by the Earth's surface. Additionally, 78 W m^{-2} of solar radiation is absorbed by the atmosphere. This leaves 102 W m^{-2} of total reflected solar radiation being lost to space.

For the Earth to maintain energy equilibrium, the outgoing terrestrial radiation must balance the net incoming radiation. Of the outgoing energy, 238.5 W m^{-2} is emitted as terrestrial radiation, comprising 187 W m^{-2} emitted directly by the atmosphere and 51.5 W m^{-2} emitted through the atmospheric window.

At the surface, 396 W m^{-2} of terrestrial radiation is emitted, of which 333 W m^{-2} is returned as downwelling radiation due to greenhouse gas effects. The net upward loss includes 17 W m^{-2} transferred as thermals, 80 W m^{-2} through evapotranspiration, and 63 W m^{-2} lost as radiation. This intricate energy balance results in a slight net absorption of 0.9 W m^{-2} , which contributes to ongoing global warming.

The spatial and temporal distribution of solar energy varies with Earth's orbit, rotation, and axial tilt, leading to seasonal differences. Polar regions experience extreme seasonal contrasts due to prolonged periods of sunlight or darkness, while tropical regions maintain relatively consistent solar input year-round.

The interaction between the Earth's components—atmosphere, oceans, and ice—plays a crucial role in moderating the climate (see Section 1.4). The oceans, covering 71% of Earth's surface, act as a massive heat reservoir, redistributing solar energy from equatorial to polar regions through currents and atmospheric interactions. Sea ice, covering up to 10% of the ocean during winter, acts as both an insulator and a reflector, influencing energy exchanges and ocean circulation. These dynamics are further impacted by phenomena like the El Niño/Southern Oscillation (ENSO) and the North Atlantic Oscillation (NAO) (see Section 1.4.2), which illustrate the interconnection of the climate system on regional and global scales (the so-called **teleconnections**).

1.1.5 The General Circulation of the Atmosphere

Since heated air tends to rise and low-level air must flow in to replace the risen heated air, the relative heating and cooling of different areas in the Earth's surface plays a significant role in driving local winds and the large-scale atmospheric circulation. The atmospheric circulation can be summed up into two different contributes: the east-west motion of the *Walker Circulation* and the north-south circulation of the three-cell structure: Hadley, Ferrel and polar cells. The Coriolis effect plays a crucial role in wind deflection to the right in the Northern Hemisphere and to the left in the Southern Hemisphere explaining the formation of trade winds, westerlies, and polar easterlies.

An idealized scheme of the aforementioned circulation pattern is displayed in Figure 1.3.

The Walker circulation

The Walker circulation refers to the equatorial Pacific and involves rising air over the region of Indonesia and descending air over the eastern Pacific. It was examined following the discovery of strong negative correlation between surface pressure anomalies in the two regions. Variations in the strength of this circulation produce a large scale fluctuation with an irregular period, known as Southern Oscillation.

The three-cell structure

The tropical **Hadley cell** is driven by solar heating, causing rising motion near the Equator, then by the release of latent heat as the rising air leads to precipitation in the rising-air

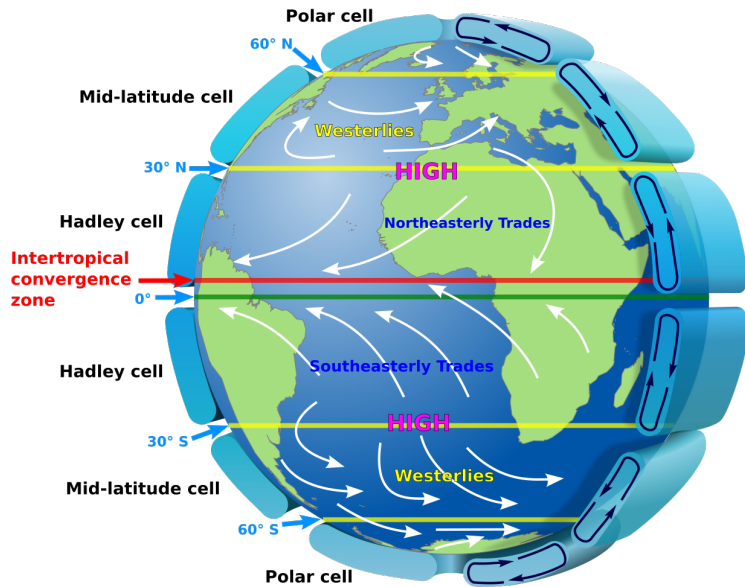


Figure 1.3: Idealised depiction (at equinox) of large-scale atmospheric circulation on Earth. Taken from [Wikipedia](#).

branch of the cell. This rising-air branch of the Hadley cell is not centered consistently on the equator but migrates north & south. Moreover, the strength of the Hadley circulation varies with longitude, being strongly affected by such factors as whether the underlying surface is land or ocean. After rising near the Equator, the air in the Hadley cell moves poleward, sinking near 30°N and 30°S and thereby generating belts of surface-level high pressure near 30°N and 30°S. Since the sea level pressure is low, the high pressure produced by the sinking air at about 30°N and 30°S creates a surface pressure gradient leading to the movement of a portion of the sinking air back toward the low pressure near the equator. The region of low-level convergence toward the bottom of the rising-air branch of the Hadley cell is called the *Intertropical Convergence Zone* (ITCZ). The position of the ITCZ shifts with the seasons, moving north during the Northern Hemisphere's summer and south during its winter. This seasonal movement affects global wind and rainfall patterns, contributing to phenomena like monsoons.

In the mid-latitude **Ferrel cell**, termed indirectly because of having rising air in its cooler branch, the low-level flow is toward the poles, away from the relatively high pressure produced by the descending arms of the Hadley and Ferrel cells at about 30° latitude and toward the relatively low pressure at about 60° latitude.

The **polar cell**: strong radiational cooling near the poles, causes polar air to become cold and dense, which in turn causes it to sink. Thus there is relatively high pressure at the pole, which, combined with the low pressure near 60°N and 60°S discussed in connection with the rising-air branch of the Ferrel cell, produces surface flow equatorward from the pole. This polar cell is extremely weak, although it remains detectable in time averages of the air circulation.

Alterations of the seasonal patterns: Breeze and Monsoons

In reality, the atmospheric circulation is more complex than what the aforementioned three-cell model suggests. It exhibits significant temporal and spatial variations due to factors like land/sea contrasts, topography, and changes in solar heating. While the model serves as a foundational framework, modern climate science relies on satellite data and simulations for a detailed understanding of global atmospheric dynamics.

Let's see an example of wind patterns driven by differences in heating between land and

water surfaces acting at the local scale, the **Breeze** and at the large scale, the **Monsoons**.

- **Sea Breeze** (Daytime): During the day, land heats up faster than water, causing air over the land to rise and creating a low-pressure zone. Cooler, denser air from over the sea flows in to replace it, generating a breeze from sea to land.
- **Land Breeze** (Nighttime): At night, the land cools faster than water, creating a high-pressure zone over the land. Air flows from the land to the sea, forming a weaker land breeze.
- **Winter Monsoon**: In winter, the land cools faster than the ocean, forming a high-pressure zone. Cold, dry air flows outward from the land to the sea, leading to dry weather conditions over most of South Asia.
- **Summer Monsoon**: Similar to a large-scale sea breeze, during summer, land masses (like South Asia) heat up more quickly than the surrounding oceans. This creates a low-pressure zone over land, drawing in moist air from the Indian or Pacific Oceans. The moisture-laden air rises and cools, resulting in heavy rainfall, particularly over mountain ranges like the Himalayas and Ghats.

Key Differences: while land/sea breezes are localized and operate on a daily cycle, monsoons occur over larger areas and are seasonal, driven by shifts in the Intertropical Convergence Zone (ITCZ). Monsoons involve additional complexities, including the influence of upper atmospheric circulations, such as the jet stream. The Asian monsoon, particularly over South Asia, is the most prominent example, crucial for regional agriculture and ecosystems. However, its dynamics are far more complex than those of simple land and sea breezes.

1.1.6 The time averaged zonal general circulation

The time-averaged circulation, computed from ERA5 Reanalysis data, shows westerly mid-atmosphere jets in the subtropical regions of both hemispheres. These jets reach a maximum around the 200 mbar level (~ 12 km) and extend to the surface in the mid-latitudes, while easterly flows dominate the equatorial zone. The jets exhibit a strong seasonal cycle, with accelerated jets in winter and weaker jets in summer. There is a seasonal poleward migration of the jet cores, with the winter season showing more concentrated and intense maximums. The Southern Hemisphere's winter jet is broader than its Northern Hemisphere counterpart, both linked to the stratospheric flow above.

The stratosphere also exhibits strong jets with a stronger seasonal cycle, where easterlies replace westerlies as the seasons change. In the meridional circulation, low-level convergence occurs at the equator, with high-level divergence. The InterTropical Convergence Zone (ITCZ) oscillates between 15°N and 5°S , influenced by the seasonal cycle of the sun.

Temperature decreases with latitude due to radiation balance, with the equator receiving more solar radiation than the poles. The temperature decreases with height in the atmosphere, though the lapse rate is less than adiabatic, indicating a generally stable atmosphere. There is a strong latitudinal temperature gradient, which weakens with altitude and reverses in the upper atmosphere and stratosphere, due to radiation absorption by ozone and other components in the lower stratosphere.

The reversal of the meridional temperature gradient aligns with the zonal wind structure, showing positive shear in the troposphere and negative shear above, consistent with thermal wind balance. Water vapor, measured as specific humidity, is concentrated in the lower atmosphere and the equatorial region, with significant dryness at higher altitudes. The atmosphere's moisture content decreases with altitude due to the Clausius-Clapeyron relation, which links water vapor pressure to temperature. tor, moist air contains 12 g–15 g of water per kg of air.

Specific humidity follows the seasonal cycle of the sun, shifting latitudinally. The maximum is located around 5°S in December–February (DJF) and around 10°N in June–July–August (JJA). The winter hemisphere is more moist at the surface than the summer, though values in the winter are smaller than in the equatorial zone, reaching up to 8 g kg^{-1} .

1.1.7 The horizontal general circulation & wind

The climatological geopotential height at 200 mbar shows deviations from a zonally symmetric circulation, particularly over the east coasts of continents, downstream from major mountain ranges like the Rockies and Himalayas. These features are clearer with specialized projections, highlighting the winter atmospheric pattern. While geopotential height can approximate wind flow in mid-latitudes, wind analysis is more useful in low latitudes.

At 200 mbar, winter jet streams are strong in both hemispheres, especially over Asia, with the Asian jet reaching velocities over 70 m s^{-1} . The Southern Hemisphere jet is weaker. In summer, westerly jets are weaker, and easterly jets dominate the tropics. The Indian Ocean sees a strong easterly flow in summer, leading to divergence over South America and Indonesia.

The meridional wind shows alternating poleward and equatorward patterns in winter, with large deviations in the Pacific–North American sector and East Asia. In summer, winds weaken but remain stronger in the Southern Hemisphere. Near the surface, the zonal wind is stronger over oceans and weaker over land, with easterlies in the subtropics, except in the Indonesian region, where westerlies prevail. The equatorial Pacific shows a convergence zone.

During JJA, the seasonal cycle strengthens winter wind features, with strong westerlies in the Indian Ocean signaling the start of the South Asian Monsoon. The meridional wind shows an equatorward flow along continent coasts, intensifying in summer, and reversing along the Somali coast.

At the 850 mbar level, trade winds dominate the equatorial Pacific, shifting with the ITCZ's seasonal cycle. The Asian Summer Monsoon is visible in the Indian Ocean, forming a large gyre from East Africa to the Indian subcontinent, crucial for understanding low-level atmospheric and oceanic interactions.

1.1.8 Mean Sea Level Pressure and The Sea Surface Temperature

Mean Sea Level Pressure (MSLP) is a key parameter in describing atmospheric circulation. It represents the atmospheric pressure adjusted to mean sea level, though its usefulness is limited in areas with significant mountains, like the Rockies, Himalayas, and Antarctica, where the concept of "sea level" is effectively underground. Outside these areas, MSLP provides a good representation of atmospheric mass distribution. High MSLP areas correspond to mass accumulation, particularly in the subtropics, where high-pressure systems are common in both summer and winter.

Near-surface temperatures, typically measured 2 m above the ground, reflect the seasonal and geographical variation in temperature. Over oceans, they follow sea surface temperature (SST), but land areas show significant seasonal changes. Northern continents are colder than the oceans at the same latitude, and coastal regions also experience temperature differences, with west coasts being milder than east coasts. In winter, high pressure tends to remain over land while low pressure develops over the oceans, reversing in summer. The intertropical zone sees high-pressure centers shifting with the seasons, while the Southern Hemisphere features a more symmetric pattern, with a ring of low pressure around Antarctica.

The seasonal cycle is evident in the shift of high-pressure areas in the tropics, moving latitudinally with the changing seasons. The meridional distribution of sea level pressure shows high pressure in the tropics, with low pressure areas near the equator and in the mid-latitudes. In the Southern Hemisphere, the pressure gradients are stronger and more pronounced, with tropical pressure maxima shifting seasonally.

Sea Surface Temperature (SST) shows strong north-south gradients, with polar regions being cold and the equator generally warm. However, notable deviations from zonal symmetry occur near continental east coasts, particularly in the equatorial Pacific, where cold water intrudes at the equator in the East Pacific, contrasting with the warm waters of the West Pacific. These temperature differences highlight significant gradients in SST along the equator

1.1.9 Energy balances in the atmosphere

At the top of the atmosphere, the energy balance is composed of the compensating fluxes between the incoming solar radiation and the outgoing thermal radiation from the Earth. The solar radiation will be modulated by the reflectivity caused by the atmospheric cloud and in smaller part by the molecular components of the atmosphere itself. The thermal radiation will be modulated by the absorption properties of the atmosphere and its constituents. Both will be affected by the circulation and ultimately by the atmospheric flows.

The net balance shows a surplus of radiative flux in the subtropical region and a deficit in the polar regions. The global radiation budget can be obtained by integrating over the surface of the Earth the radiative fluxes.

At the surface, the energy balance involves more processes. There is also here a net solar radiation flux, modulated by the albedo of the surface and of the atmosphere, and a net thermal flux, obtained as the balance between the radiation emitted by the surface and the downward flux coming from the bulk of the atmosphere. Then there is a sensible heat flux caused by the turbulent vertical motion that carries away heat through mechanical agitation and the latent heat flux that represents the heat necessary for the evaporation of water from the surface. Because of the extent of the ocean, the latent heat flux is an important element of the budget.

In addition, we can look at the total cloud cover which is essentially the aggregated quantity of clouds at various levels. This is the quantity that is intuitively linked to the observation of a “cloudy sky”. In general, clouds are present over a vast surface of the globe. Some areas show a persistent absence of cloudiness over the entire year, such as the Sahara desert, part of the Arabian peninsula, Australia, and South Africa. Other areas instead show a strong seasonal cycle, with different cloud cover in different seasons. It is interesting to note that the seasonal cycle takes different characteristics in different areas. In the mid-latitudes cloud cover is larger in the local hemispheric winter than in the summer.

Looking at the zonal profile of the clouds, it is evident that major concentrations are related to the equator and middle/high latitudes.

1.2 Oceans

Oceans, covering approximately 71 % of Earth’s surface, play a crucial role in global climate systems by storing and transferring heat, nutrients, and momentum. The interaction between the atmosphere and oceans significantly impacts weather and climate patterns. These bodies of water contain an estimated $1350 \times 10^6 \text{ km}^3$ of water, predominantly found in the Pacific, Atlantic, Arctic, and Southern Oceans, with an average depth of about 4000 m.

Surrounding continents are continental shelves, shallow areas that extend outward for several kilometers before dropping sharply at the continental slope into the deep ocean floor. The ocean floor itself is varied, featuring features like underwater mountains, ridges, trenches, and smooth sedimentary basins.

The oceans redistribute solar energy from equatorial to higher latitudes. As water warms at low latitudes, it absorbs significant amounts of solar heat. This heat is released into the atmosphere in the form of latent heat and longwave radiation as water cools or condenses,

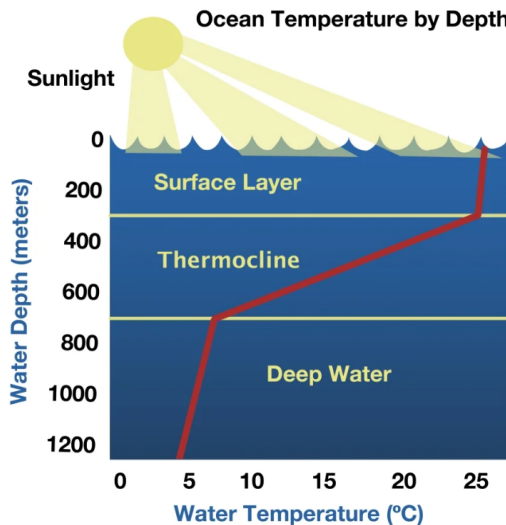


Figure 1.4: Ocean temperature by depth.

influencing global atmospheric circulation. Ocean currents further distribute this heat, balancing regional temperatures and aiding in climate regulation (see e.g. Section 1.2.4).

1.2.1 Oceanic Composition

Seawater is not just water but a mixture containing various dissolved salts, with an average salinity of 35 grams per kilogram of water. This salinity largely comes from chloride, sodium, and sulfate, accounting for the majority of dissolved material. Salinity levels, however, vary globally. The Arctic Ocean shows lower salinity ($\sim 29\%$), influenced by melting ice and freshwater inflows, while the subtropical Atlantic has some of the highest salinity ($\sim 37.5\%$), due to high evaporation and low precipitation. These variations affect density, which in turn drives ocean circulation and temperature dynamics. Overall, oceans are not only a storage medium for heat and nutrients but also critical in redistributing energy across the planet, moderating climate, and supporting ecosystems. Their interaction with atmospheric processes underscores their integral role in Earth's environmental systems.

1.2.2 Thermal structure

For a more in-depth analysis of the Thermal structure of the Ocean see e.g. [here¹](#).

Surface temperature

Range: -1°C (polar regions) to 20°C – 30°C (tropics). Seasonality: temperatures align in east-west zonal patterns, with exceptions like:

- Tropical Pacific: western regions warmer than eastern regions due to currents.
- Gulf Stream: transports warm water northeast, moderating European climates.

Vertical temperature

- Mixed Layer (0 m–30 m in summer): warmed by sunlight and mixed by winds.
- Thermocline (200 m–1000 m): sharp temperature gradient separating surface water from deeper layers.

¹Goal: include the analysis in the notes.

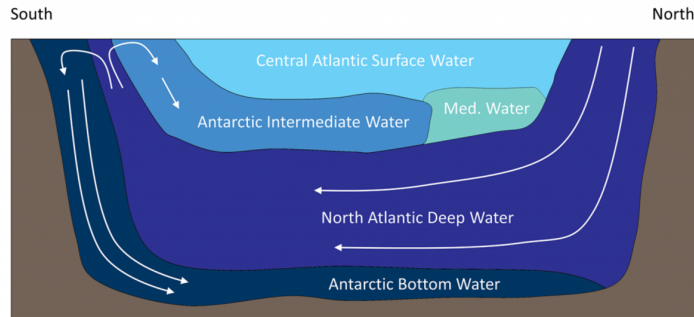


Figure 1.5: The major water masses of the Atlantic Ocean

- Deep Ocean ($> 1000 \text{ m}$): uniform cold temperatures (0.5°C – 1.25°C).
- Coldest water (-0.25°C) near Antarctica due to sinking dense, salty water from surface cooling and sea ice formation.

Ocean circulation is driven by temperature and salinity differences, influencing density and pressure. Surface currents are wind-driven, forming large gyres such as those in the Pacific and Atlantic Oceans. These gyres redistribute heat and nutrients, shaping regional climates and ecosystems. Deep ocean currents, part of the thermohaline circulation², involve the sinking of dense, cold water and the upwelling of warmer, nutrient-rich water, critical for sustaining marine life. Additionally, mesoscale eddies, swirling water masses (Figure 1.5), play a significant role in transporting momentum, heat, and nutrients horizontally and vertically, although their dynamics are not fully understood. These processes together illustrate the complex and vital role oceans play in regulating Earth's climate and supporting life.

1.2.3 The salinity structure of the ocean

The salinity structure of the oceans is shown in Figure 1.6. The top panel shows the salinity near the surface at a nominal depth of 5 m. We notice that there is a complex structure with low salinity (fresher) waters at the poles and progressively more saline water moving towards the Equator, but then salinity decreases again at the equator. It is probably instructive to look at the latitudinal distribution of the precipitation. We can notice that the peaks of precipitation in the midlatitude and at the Equator are correlated with the low-salinity areas, whereas the subtropical regions are regions of strong evaporation, whose signature is the high salinity of the surface waters.

The Pacific Ocean is fresher than the Atlantic or even the Indian Ocean. We can see from the map at 1000 m that sources of saline waters are marginal seas like the Mediterranean and the Persian Gulf. These areas are evaporative basins that produce water so saline that it dominates over the temperature effect and becomes denser so that we can find Mediterranean water below the surface.

The effect of the precipitation is less visible at the deeper depth of 1000 m (bottom panel of Figure 1.6), where the ocean tends to be fresher and more uniform. We are using here the same scale to give a feeling of the changes in salinity, except for the Atlantic and the east Indian Ocean, the salinity is around 34 psu. The effect of the runoff from major river systems is visible along the Atlantic coast of South America where the Amazon river discharges and in the Bay of Bengal and around Indochina from the run-off the major rivers there, the Ganges and the Mekong.

In the pictures below: on the left salinity deviations with depth, going even deeper we have to change drastically the scale. The oceans are remarkably uniform and the salinity

²<https://rwu.pressbooks.pub/web/oceanography/chapter/9-8-thermohaline-circulation/>

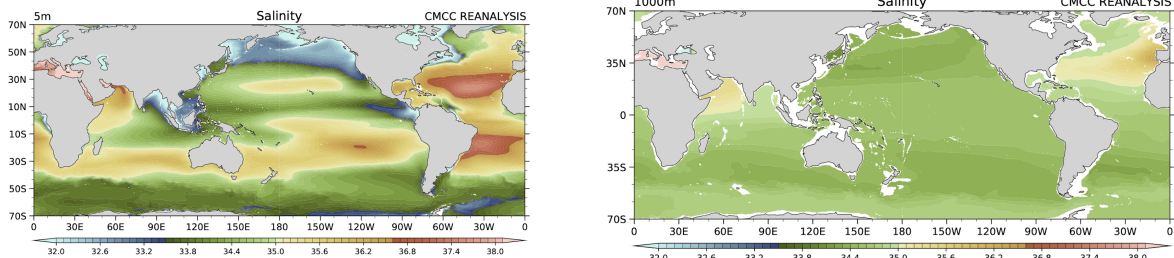


Figure 1.6: Global ocean salinity level at 5 m and 1000 m, respectively (From [CMCC reanalysis](#)).

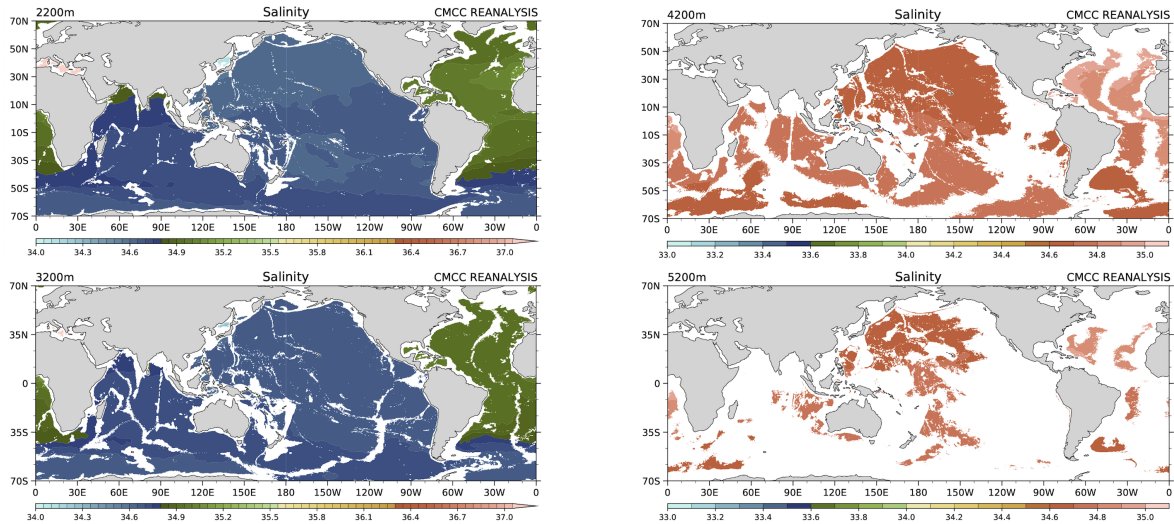


Figure 1.7: Salinity distribution in the North Atlantic at different depths from [CMCC reanalysis](#). The four panels represent depths at 2200 m, 3200 m, 4200 m, and 5200 m, respectively.

deviations are really small. On the right, Pacific and Atlantic ocean salinity.

Looking at the North Atlantic (see Figure 1.7) we notice that there is a strong salinity gradient along the North American Coast that follows roughly the pattern of the temperature gradient shown below. Strong temperature gradients are presumably to be connected to the existence of currents, but we will need to check the density, depending on the salinity later, to be sure. Anyway, Figure 1.7 is giving a strong indication of the existence of something remarkable and intense along the western boundary of the Atlantic ocean.

A similar situation exists in the North Pacific along the Japan coast (see Figure 1.8) and therefore we can start to suspect that this has to do with the presence of the continental boundary.

The previous analysis of the temperature is giving us hints of a strong vertical structure of the oceans, so it may be useful to look at the vertical distribution somewhat more in detail. Figure 1.9 shows the same section North-South section of along the longitude of 25°W , roughly in the middle of the Atlantic Ocean. The salinity follows a similar pattern as the temperature with a strong gradient approximately at the thermocline, the high salinity is confined in thin layers at the surface, but some interesting behaviour is visible below. In the Northern Hemisphere we can see the Mediterranean water penetrates at depth and actually protruding under the fresher water of Antarctic origin that is colder, but because is fresher floats over the Mediterranean water. Really cold Antarctic water reaches the bottom, filling the abyssal plains of the basin.

The Mediterranean waters are clearly visible in a longitude-depth section (Figure 1.9).

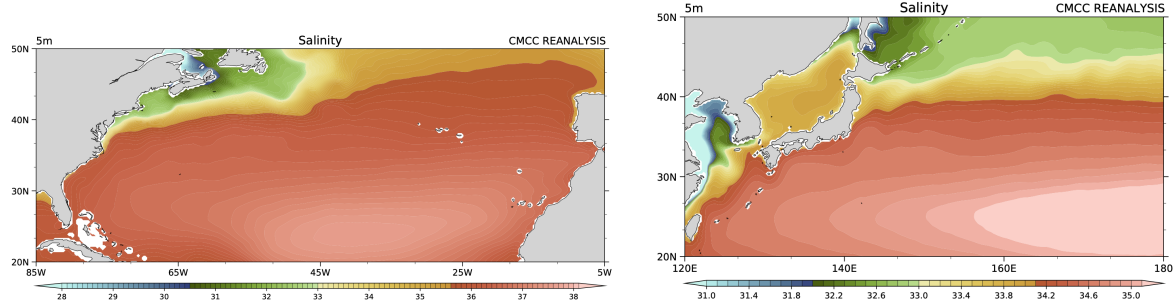


Figure 1.8: Salinity at 5 m level in North Atlantic, next to the US East Coast (left) and in the North Pacific offshore Japan's East coast. From [CMCC reanalysis](#).

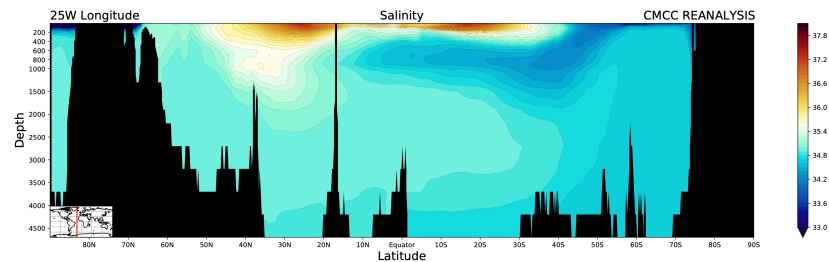


Figure 1.9: Vertical salinity profile section at 25°W longitude. From [CMCC reanalysis](#).

The saline Mediterranean water sinks to about 1000 m because it is warmer than the Atlantic but much more saline so it is denser and it reaches an equilibrium depth at about 1000 m.

The vertical structure of the Pacific Ocean (Figure 1.10 shows the salinity along the horizontal 25°N line) is different and what we see is a situation where salinity is slowly varying getting fresher toward the surface, with the thin saline water in the subtropics a clear signature of the equatorial upwelling and the Antarctic water filling the abyssal plains. The Indian Ocean is similar to the Pacific South of the Equator but North of the Equator at this longitude is fresher.

The Indian Ocean cut as a section cutting essentially through the Bay of Bengal as shown in Figure 1.11, shows a similar strong stratification, but there are only weak signs of an equatorial upwelling of cold water.

We can gain more insights in the equatorial structure by looking at a longitudinal section along the Equator in the Pacific (see Figure 1.12). Here we see the general difference between the Atlantic and the Pacific, but we also see that the salinity is following the slant of the equatorial thermocline and the equatorial upwelling in the East Pacific. The effect of the major precipitation center of ITCZ in the West Pacific is visible in fresh water at the surface in the West.

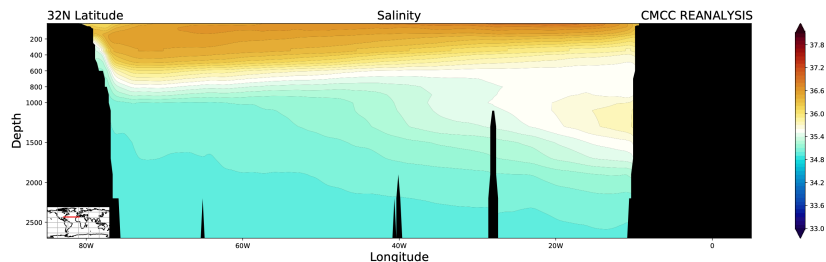


Figure 1.10: Horizontal Salinity profile section at 25°N latitude. From [CMCC reanalysis](#).

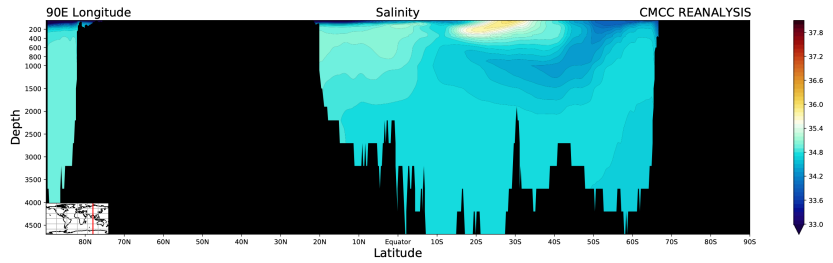


Figure 1.11: As in Figure 1.10 but for 90°E longitude. From CMCC reanalysis.

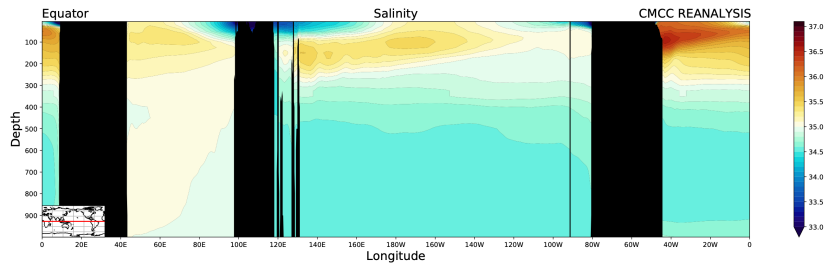


Figure 1.12: Horizontal Salinity profile section at the equator. From CMCC reanalysis.

1.2.4 Influence of the ocean

The *continentality effect* makes continental summers warmer and winters cooler than the adjacent ocean areas. The oceans have this effect because of their large heat storage capacity and because part of the energy that they retain from solar input during the summer they return to the atmosphere in the forms of sensible and latent heat and longwave radiation the following winter. Conversely, the continents have the reverse effect, strengthening the seasonal temperature contrasts

1.2.5 Ocean currents

They can transport heat from low to high latitudes. (in the Gulf Stream of the North Atlantic). This contributes to much higher winter air temperatures over mid-to-high latitude oceans than over adjacent land areas at the same latitude.

The overall basin circulation

The surface currents of the Atlantic ocean are shown in Figure 1.13. As we might have suspected from the temperature coast that reaches all the way across the North Atlantic to Europe, the Gulf Stream. Strong currents are also visible in the Equatorial area where they connect to the mid-latitude circulation forming a large circular system, the Subtropical Gyre. The South Atlantic has a similar gyre in the subtropical region, but at higher latitudes we can notice a strong westerly current cutting all along the basin, essentially along a latitude line between 40S and 50S.

The North Pacific surface circulation is shown in Figure 1.14. We can notice here again a strong current along the Western boundary of the basin that then feed into a basin wide gyre that connects to the equatorial circulation. The boundary current, known here as the Kuroshio Current, is very narrow and intense along the Japan coast, as it is also the case of the Gulf Stream in the Atlantic, and it tapers into a wide system of streams and eddies into the open ocean.

It is possible to see also local systems, like the small gyre off the Alaskan coast and similar circulation in the marginal seas, like the Sea of Okhotsk, near the Siberian coast. Their

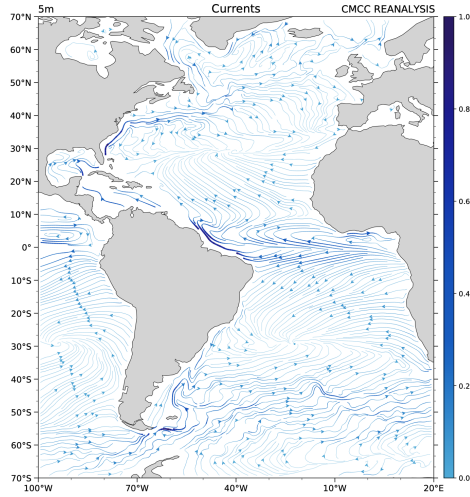


Figure 1.13: The surface circulation of the Atlantic Ocean, shown as streamlines whose color and thickness are indicating the speed of the current in m s^{-1} .

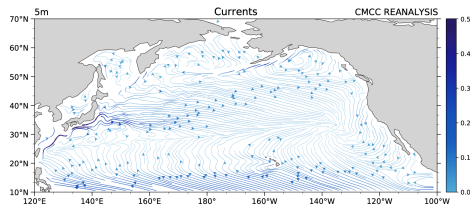


Figure 1.14: The surface circulation of the North Pacific Ocean, shown as streamlines whose color and thickness are indicating the speed of the current in m s^{-1} .

presence is remarkable as we are looking here at climatological averages over more than 40 years and so they are stable and persistent features. This is another reminder of how even relatively smaller feature in the ocean can be climatologically persistent over many years.

The circulation of the South Pacific Ocean is shown in Figure 1.15. The subtropical gyre is visible also here, but there is a weak indication of a western intensification current in the West pacific, close to the coasts of Australia and New Zealand. The strong high latitude current that we have seen in the Atlantic is also present here and evidently connect to the other basin through the Drake Passage, that is the Straits between South America and Antarctica.

The Indian Ocean circulation is shown in Figure 1.16. The Indian Ocean is confined by continental masses in the north, so it is mostly composed of the equatorial region and the midlatitudes are all in the Southern Hemisphere. The subtropical gyre is present, together with features North of Madagascar. A boundary current develops on the African coast, The westerly current in the southern mid-latitudes is visible also here, strong and with a vigorous eddy field.

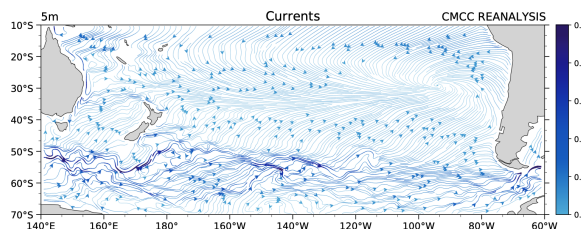


Figure 1.15: The surface circulation of the South Pacific Ocean, shown as streamlines whose color and thickness are indicating the speed of the current in m s^{-1} .

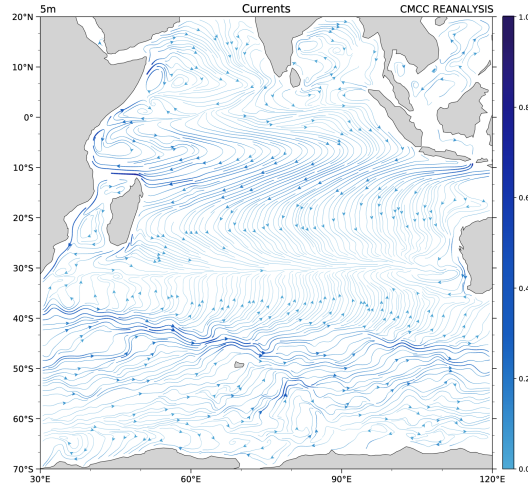


Figure 1.16: The surface circulation of the Indian Ocean, shown as streamlines whose color and thickness are indicating the speed of the current in m s^{-1} .

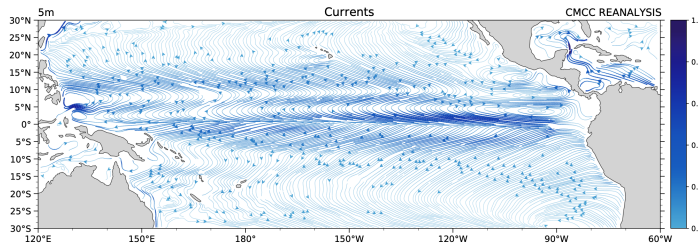


Figure 1.17: The surface circulation of the Equatorial Pacific Ocean, shown as streamlines whose color and thickness are indicating the speed of the current in m s^{-1} .

At this point we can suspect that there is probably a continuous ring of currents around Antarctica and this can be confirmed by the bottom panel of Figure ?? that shows the entire extent around a longitude circle of the current, known as the Antarctic Circumpolar Current. It is a strong, highly turbulent system that connects all the Ocean Basins.

The equatorial circulation

The Equator is a special place for the atmosphere and so it is a special place also for the Oceans. The circulation in this area is strongly coupled with the atmospheric circulation and it is often characterized by both westerly and easterly currents and by special behaviours right at the Equator line. Furthermore, it is also very different from ocean to ocean.

The equatorial current system in the Pacific Ocean is shown in Figure 1.17. It is a complex system composed of two easterly currents, the North and South Equatorial currents, sandwiching the westerly Equatorial countercurrent. It is possible to notice that at the Equator the currents are strongly easterly and diverging, leading to the emergence of upwelling at the Equator by Ekman transport.

The complexity of the equatorial current system can be further appreciated by looking at the vertical section of the zonal current at the Equator. A strong westerly current below the surface, slanting from the West Pacific to the East Pacific, is visible at depth between 200 and 300m. The speed is in excess of 1 m s^{-1} and it gets progressively shallower in the East.

It is however part of an alternation of westerly and easterly currents that become progressively weaker as they get deeper. They are centered almost perfectly at the Equator, as it can be seen in Figure 1.18. The latitudinal position of the undercurrent is very tightly controlled by rotational effects and it precisely tracks the position of the equatorial line.

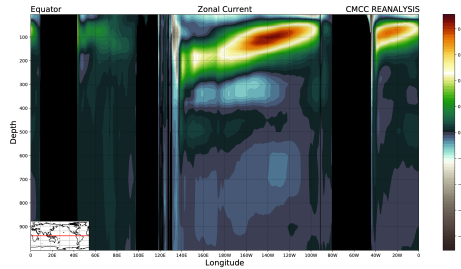


Figure 1.18: Alternation of westerly and easterly currents. The vertical section of the zonal current at the Equator in the Global Ocean from the surface to 1000 m. Units are m s^{-1} .

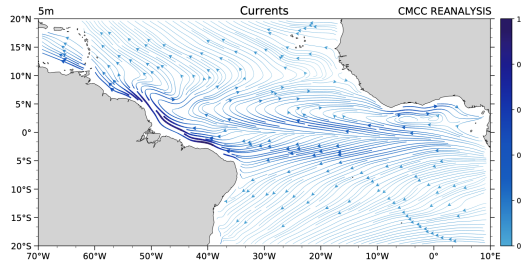


Figure 1.19: The equatorial Atlantic current systems at the surface. Units are m s^{-1} .

The equatorial Atlantic Ocean surface circulation (Figure 1.19). It is possible to see the easterly South Equatorial Current that is straddling the Equator between 5°S and 5°N . The North equatorial Countercurrent is westerly and it covers the area between 5°N and 10°N , and the weaker North Equatorial Current is located at northern latitudes. The equatorial flow is divergent and also in this case we can presume the existence of upwelling at the Equator. A strong coastal current is visible as the Guinea Current, in the Gulf of Guinea. The South Equatorial Current feeds into the North Brazilian Current that then flows northward along the South America coast, taking different names as it finally emerges as the Caribbean Current in the Caribbean sea. A similar structure of alternating westerly and easterly undercurrents exist also in the equatorial Atlantic (Figure 1.19), but it is weaker and only the first westerly maximum is well visible. It is also slanting towards the East, but the maximum is reached more towards the western boundary of the basin with respect to the Pacific Ocean. The deeper easterly jets are also much less weak. The undercurrents jets are essentially absent in the Indian Ocean.

The Gulf Stream

The current system of the Gulf Stream is one of the major feature of the global ocean circulation.

The Kuroshio

The current system of the Kuroshio is one of the major features of the global ocean circulation³.

1.3 Ice

Sea ice covers about 7% of Earth's oceans and plays a critical role in the global climate system, acting as a barrier between the atmosphere and the ocean. It forms when seawater cools

³Figures to cite.

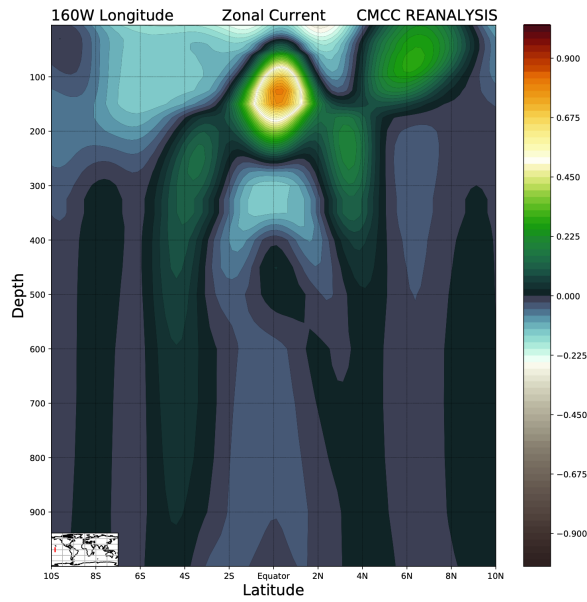


Figure 1.20: Structure of currents and undercurrents as latitude-depth section of the zonal current at the Equator for the Pacific Ocean at 160°W longitude from the surface to 1000 m. Units are m s^{-1} .

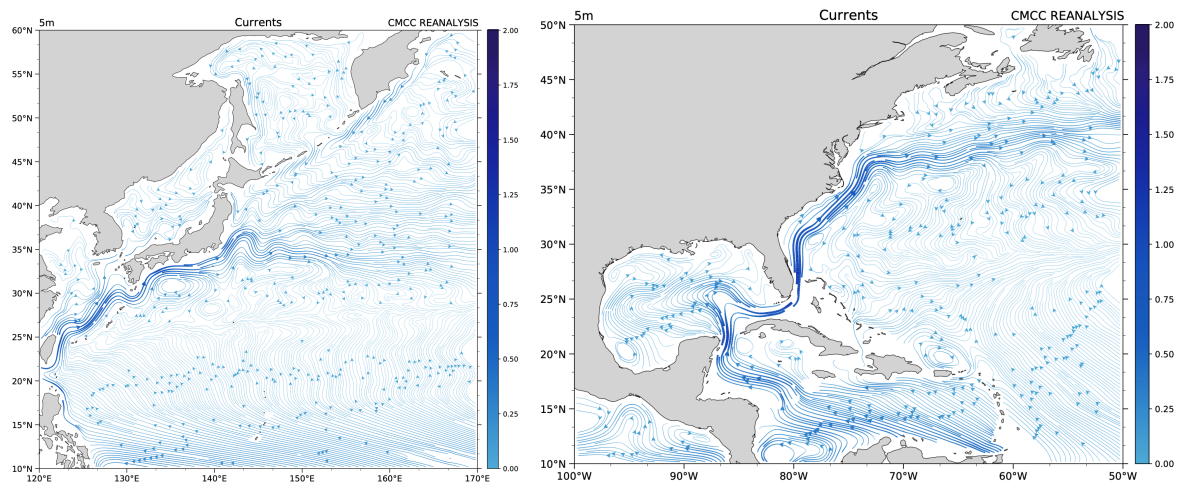


Figure 1.21: On the left, the circulation of the Kuroshio at the surface, shown as streamlines whose color and thickness are indicating the speed of the current.

On the right The circulation of the Gulf Stream at the surface, shown as streamlines whose color and thickness are indicating the speed of the current, for both measured in m s^{-1} .

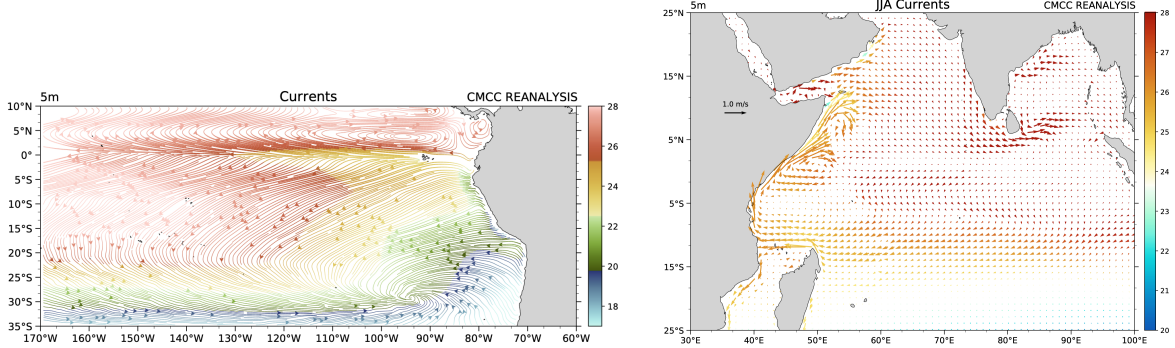


Figure 1.22: On the left The upwelling zones in the East Pacific. The streamlines color is proportional to temperature and the thickness is indicating the speed of the current in m s^{-1} . The seasonal variation of the Somali current in Summer. The arrows color is proportional to temperature, units are m s^{-1} .

below its freezing point, creating ice floes that are often cracked and shifted by environmental forces. Despite its compact appearance, sea ice is dynamic and never fully covers open water areas due to constant movement and deformation.

In the Southern Hemisphere, sea ice extends seasonally from about $3 \times 10^6 \text{ km}^2$ in summer to $18 \times 10^6 \text{ km}^2$ in winter, covering around 7% of the Southern Ocean at its peak. The ice can reach as far as 60°S during winter, particularly in the Weddell and Ross Seas. However, it tends to be less compact compared to the Arctic, largely due to divergent winds and the influence of ocean currents. By contrast, in the Northern Hemisphere, sea ice ranges from $7 \times 10^6 \text{ km}^2$ in summer to $15 \times 10^6 \text{ km}^2$ in winter, making up about 10% of the ocean area during its maximum extent. The Arctic Ocean forms the core region of sea ice, with thick polar caps and thinner ice in surrounding seas like the Bering Sea and the Sea of Okhotsk. Ice can also drift into the North Atlantic through the Labrador and Greenland seas. The formation of sea ice depends on several factors. Salinity plays a crucial role, as higher salinity lowers the freezing point of seawater. In regions with salinity levels above 24.7%, convective mixing occurs as dense, salty water sinks, delaying the freezing process. Under calm conditions, supercooling can allow water to remain liquid below its freezing point until ice crystals form, which then accelerate the freezing of surrounding water. As the ice thickens, it insulates the ocean below, reducing heat loss and slowing further growth.

Sea ice melts during summer, particularly in the Arctic, where increased sunlight and prolonged daylight accelerate the process. Melting can occur at rates of about 40 mm per day, with melt ponds and drainage channels forming on the surface. The loss of ice is further aided by tidal forces and storms, leading to disintegration near coastlines and open water areas. By late summer, much of the peripheral sea ice in the Arctic disappears, leaving only the central ice pack.

Sea ice properties vary greatly between the Arctic and Antarctic regions. In the Arctic, central ice thickness typically ranges from 2 to 4 meters, with thinner ice in peripheral seas (0.5 to 1 meter). Antarctic icebergs are far larger, often exceeding 600 meters in thickness. Ice density, generally between 880 and 910 kg/m^3 , allows it to float. The topography of sea ice includes ridges and rubble zones formed by colliding ice sheets, with some ridges extending 10 to 15 meters below the surface.

The movement of sea ice is also an important factor in ocean circulation and climate. In the Arctic, the Beaufort Gyre and the Transpolar Drift Stream transport ice across the Arctic Basin, eventually exiting through the Fram Strait into the North Atlantic. This ice contributes to cold currents like the East Greenland Current. In the Antarctic, ice drifts clockwise in the Weddell Sea, eventually melting in warmer waters and transporting freshwater to lower latitudes.

Overall, sea ice is a vital component of Earth's climate system. It influences heat exchange between the ocean and atmosphere, regulates salinity and density in ocean waters, and contributes to the broader dynamics of polar and global ocean circulation. Its seasonal cycles and properties make it an essential focus for understanding climate change and its impacts.

1.4 Interconnections between atmosphere, ocean and ice

Important transfers of energy, mass, momentum occur between the oceans and the atmosphere and are greatly modified by the presence of sea ice.

1.4.1 Atmosphere effect

Wind forcing is a prime driver for upper ocean circulation and thereby impacts deep ocean circulation as well, and for sea ice thereby impacting its motions and location. In addition, air temperatures and moisture contribute to determining the energy fluxes across the interface between the atmosphere and surface, contributing to ice maintenance, growth and melt and to the temperature distribution in the ocean and water velocity. Fridtjof Nansen noted that sea ice does not drift in the direction of the wind but at an angle of 20°–40° to the right due to the Earth's rotation and speculated that the motions in the water beneath sea ice deviate even more; the motion of each water layer deviates slower and farther to the right to the layer above and Ekman proved it mathematically adding that these influence stops at a depth of about 200 m (see e.g. Section 3.1 of Zanotti, 2023).

1.4.2 Ocean effect

Ocean has a significant impact on the other two components. It is essentially a limitless moisture source and supplies the majority of atmospheric water vapor. The ocean land contrast exerts a major control over the distribution of evaporation over the global precipitation. The thermal inertia of the ocean results in a much lesser seasonal temperature range at the open ocean surface than at a land surface or a sea ice surface. This creates a lesser atmospheric temperature range over open ocean than over land or sea ice, as cold winter air is warmed by the underlying ocean and warm summer air is cooled. Since the ocean also absorbs a significant amount of the atmosphere's carbon dioxide (CO₂), it also helps to slow the buildup of atmospheric CO₂.

The oceans contribute significantly to the poleward transport of heat, by means of ocean currents. This transport influences the heat balances in both high and low latitudes and the average temperature gradient between the equator and the poles. The temperature distribution of the ocean surface is the prime determinant of the sea ice distribution, because, in general, ice forms where the water temperature has reached the freezing point. Similarly, the ocean salinity distribution is important to the formation of sea ice, because the salt content of the water affects the freezing temperature. Once ice is formed, warm currents entering an ice-covered region tend to melt the ice cover, and cold currents moving away from the ice region tend to carry ice with them.

El Niño/Southern Oscillation (ENSO)

This is an example of atmosphere/ocean interconnections one of the major large-scale patterns. The El Niño and Southern Oscillation phenomena were originally examined separately, before their close interconnection became apparent.

El Niño originally referred to a seasonal warming of the waters along the coast of Peru, frequently occurring shortly after Christmas. The term is now generally restricted to large-scale warming events, extending well into the central equatorial Pacific. The episodes can last many

months, and do not necessarily begin near Christmas. **The Southern Oscillation**, characterized by consistent sea level pressure, temperature, and precipitation changes in the South Pacific, was first discussed by Walker who found an alternating pressure pattern involving the normal southeast Pacific high pressure and the low pressure region near the Indian Ocean and western Pacific regions.

Under normal conditions (non–El Niño), there is a strong sea surface temperature difference between the warm western Pacific and the cooler eastern Pacific, caused by upwelling along South America’s west coast driven by east-to-west trade winds. This setup creates a convection cycle where air rises over the warm western Pacific, leading to heavy rainfall, and sinks over the cooler eastern Pacific, forming an east-west Walker circulation.

During El Niño, the trade winds weaken, reducing upwelling along the South American coast. This leads to warmer sea surface temperatures in the eastern Pacific, disrupting the temperature gradient. As a result, air rising and rainfall patterns shift eastward, cooling the western Pacific and causing significant climate effects. For example, the Indonesian-Australian region may experience drought, while wetter conditions occur farther east.

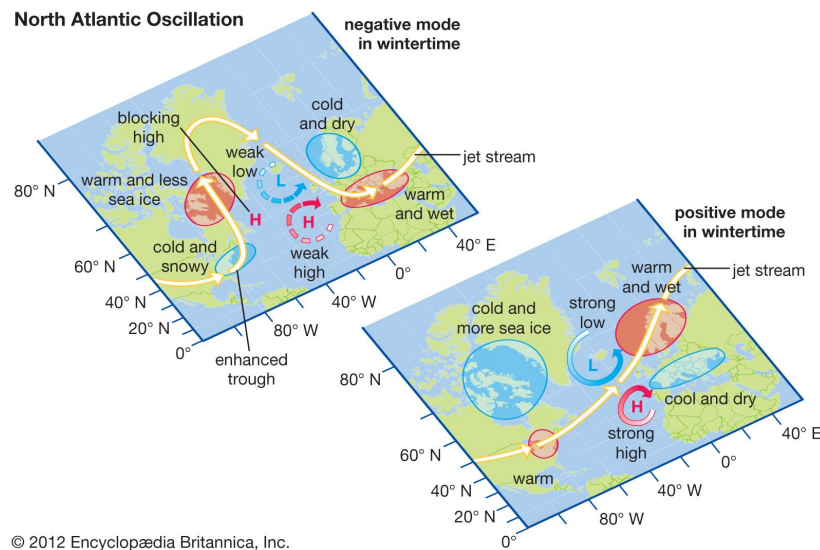


Figure 1.23: The typical path of the polar-front jet stream during negative and positive modes of the North Atlantic Oscillation. Taken from [Encyclopedia Britannica](#)

North Atlantic Oscillation (NAO)

The North Atlantic Oscillation (NAO) is a pressure oscillation measured by the sea level pressure difference between Iceland and the Azores, reflecting the strength of the Icelandic low-pressure system and the Azores high-pressure system. (although sometimes it is indexed instead by the pressure difference between Newfoundland and Lisbon, Portugal, or between Iceland and Lisbon). It has both short-term and long-term variations, significantly affecting North Atlantic climate patterns. Positive NAO phases strengthen the Icelandic low pressure, resulting in colder winters in eastern North America, warmer and wetter conditions in western Europe, reduced sea ice near Greenland and Scandinavia, and increased sea ice in Baffin Bay and the Labrador Sea.

NAO impacts extend to global teleconnections, including influences on Russia, the Indian monsoon, and ocean temperatures. The positive NAO phase is associated with a tripolar sea surface temperature pattern: a cold anomaly in the subpolar North Atlantic, warm anomalies near Europe, and a cold subtropical anomaly near the Equator. The Gulf Stream further propagates these anomalies toward Europe, enabling atmospheric feedback and improving

predictability of NAO patterns. The interaction between the ocean and the NAO remains a key area of research.

1.4.3 Ice

The presence of sea ice has numerous climatic consequences, influencing the temperature and circulation patterns of both the atmosphere and the oceans. Sea ice lessens the amount of solar radiation absorbed at the ocean's surface: only about 20%–50% of the incident solar radiation is absorbed, the rest being reflected to space and is therefore lost, while without the ice, typically 85%–95% is absorbed. It serves as a strong insulator, restricting exchanges of heat from 10^2 W m^{-2} to 10^3 W m^{-2} from the ocean to the atmosphere, to 10 W m^{-2} to 20 W m^{-2} ; mass, momentum, and chemical constituents between the ocean and atmosphere. In winter, ice cover enhances polar cooling by increasing temperature gradients between the poles and the equator, intensifying atmospheric circulation. However, stronger circulation brings warm air into polar regions, reducing these gradients and creating a negative feedback, making the overall effect on atmospheric circulation uncertain. In summer, ice acts as a thermal insulator, reducing heat transfer from the atmosphere to the ocean. Its high albedo also reflects solar radiation, limiting heat absorption and increasing the net heat gain in polar oceans. These seasonal dynamics highlight the complex role of ice in the climate system.

Another aspect of the insulation is the lessened evaporative transfer to the atmosphere in the presence of ice cover, resulting in reduction of moisture available for cloud formation, rain and snow.

The freezing and melting of sea ice influence seasonal and regional climates by moderating temperature extremes. Ice formation releases heat, while melting absorbs heat, facilitating a net equatorward transport of heat and salt from polar regions. During ice formation, salt is rejected into the underlying ocean, increasing the salinity and density of the mixed ocean layer, which can lead to deep convection and the formation of bottom water that drives global ocean circulation. This process is most significant at the edges of ice packs, where winds create open water that freezes rapidly, enhancing local ice production. Approximately one-third of bottom water originates from ice formation along ice margins. These dynamics connect ice processes to global climate systems, influencing both local and large-scale ocean circulation.

Chapter 2

Fundamental equations and processes

Last updated: 2024-12-06

Source file: [chapter-fund-eqs-processes.tex](#)

The atmosphere and the ocean are both vast and dynamic systems that behave as fluids under the influence of a rotating planet. Although their physical properties differ—air being compressible and water being nearly incompressible—their motions can be described using the principles of fluid dynamics. These principles form the basis for understanding and predicting a wide range of phenomena, from local weather patterns to global climate dynamics.

In this chapter, we explore the fundamental equations that govern the behavior of these fluid systems. Starting from the basic conservation laws of momentum, mass, and energy, we show the governing equations for atmospheric and oceanic motion. Due to the complexity of these systems, certain approximations are often applied to make these equations tractable. These approximations include the hydrostatic approximation, the shallowness approximation, and the neglect of specific higher-order terms. Such simplifications allow us to focus on the dominant processes and forces shaping the dynamics of the atmosphere and the ocean.

We will discuss the mathematical framework and coordinate systems used to describe these systems, followed by the equations of motion and key approximations. Later sections will delve into the physical processes such as radiation, moisture, and hydrology that interact with the dynamics of the atmosphere and ocean.

2.1 Background

2.1.1 The Earth spherical coordinates system

The most commonly used coordinate system for the analysis of the atmosphere and the oceans is a spherical coordinate system attached to the rotating Earth (Figure 2.1). The spherical coordinates are slightly different from the usual mathematical ones as the latitude ϕ is measured from the equator and therefore it can take negative values. The longitude λ is running west to east.

The longitude is also known as the **zonal** direction whereas the latitude is also known as the **meridional** direction. Winds are identified by the direction they are coming from, so a *westerly* wind is coming *from* the West and an *easterly* wind is coming *from* the East.

Hereafter we will denote with $\Omega = \Omega \hat{\mathbf{k}}$ Earth's angular velocity vector, with $\Omega \simeq 7.29 \times 10^{-5} \text{ rad s}^{-1}$. Since this reference frame is rotating, it is necessary to add force terms in the dynamical equations (see Coriolis terms in Equation 2.3).

2.1.2 Rates of change of fluid properties over time: Eulerian vs Lagrangian description

In fluid dynamics, there are two primary perspectives for describing the motion of fluids and their properties: the Eulerian and the Lagrangian.

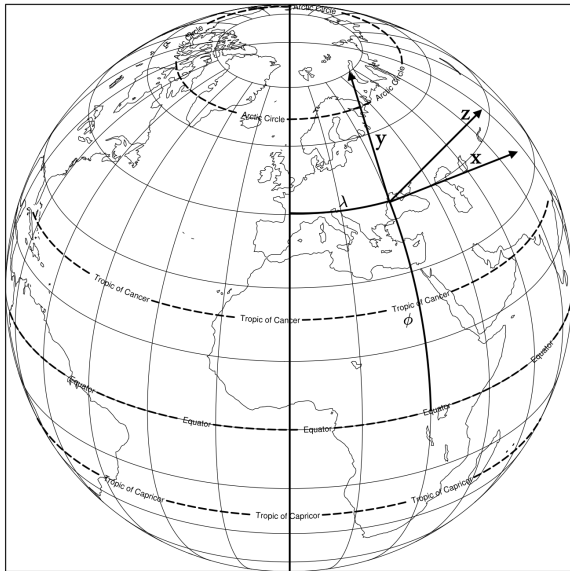


Figure 2.1: 3D Spherical coordinate system.

The **Eulerian description** focuses on specific points in space through which the fluid flows. Changes in fluid properties, such as velocity, temperature, or pressure, are observed at these fixed spatial locations over time. This is analogous to standing on a bridge and watching water flow underneath. This perspective is often used in large-scale atmospheric and oceanic studies.

In contrast, the **Lagrangian description** follows individual fluid parcels as they move through space and time. It tracks changes in the properties experienced by these parcels. This is akin to floating along with the current in a boat and observing changes in the surrounding environment. This perspective is particularly useful when studying transport and mixing in fluids, such as pollutant dispersion or cloud formation.

The connection between these two perspectives is captured by the **advective derivative** - also known as *material derivative* or *Lagrangian derivative* - which describes the rate of change of a property $\phi = \phi(\mathbf{x}, t)$ as seen from the perspective of a moving fluid parcel. It combines the local rate of change (Eulerian derivative) and the transport of the property due to the fluid motion (advection). Mathematically, the advective derivative is expressed as:

$$\frac{D\phi}{Dt} = \frac{\partial\phi}{\partial t} + \mathbf{u} \cdot \nabla \phi \quad (2.1)$$

where:

- $\frac{D\phi}{Dt}$ is the advective derivative, representing the total rate of change of ϕ in a moving frame;
- $\frac{\partial\phi}{\partial t}$ is the Eulerian derivative, capturing the local rate of change of ϕ at a fixed location;
- $\mathbf{u} \cdot \nabla \phi$ is the advection term, representing the transport of ϕ by the fluid velocity \mathbf{u} .

Proof. To compute the total rate of change of a fluid property ϕ we have to consider it is evolving both in time t and in space \mathbf{x} (the fluid is moving), therefore

$$\frac{\partial\phi}{\partial t} + \frac{\partial x}{\partial t} \frac{\partial\phi}{\partial x} + \frac{\partial y}{\partial t} \frac{\partial\phi}{\partial y} + \frac{\partial z}{\partial t} \frac{\partial\phi}{\partial z} = \frac{\partial\phi}{\partial t} + \mathbf{u} \cdot \nabla \phi \quad (2.2)$$

where we have recovered Equation 2.1. □

2.2 Primitive equations

The motion of a physical system is governed by conservation laws: conservation of momentum (Equation 2.3), mass (Equation 2.7) and energy (Equation 2.8). The conservation of momentum equation will identify the forces acting on the system. The conservation of energy will identify the processes capable of changing the energy of the system, i.e. thermodynamical processes.

2.2.1 Momentum equation

The first set of fundamental equations that we encounter is the conservation of momentum, which, for a geophysical fluid correspond to the **Navier-Stokes equations**. The Navier-Stokes equations describe the motion of fluid substances like air and water. They account for forces due to pressure, viscosity, and external forces such as gravity. This set of equations is key to understanding how winds, ocean currents, and other flows evolve due to internal and external forces. In the rotating reference frame described in Section 2.1.1 the aforementioned governing equations, written along three coordinates longitude λ , latitude ϕ and vertical direction z , read:

$$\frac{Du}{Dt} - \frac{uv \tan \phi}{r} + \frac{uw}{r} = -\frac{1}{\rho r \cos \phi} \frac{\partial p}{\partial \lambda} + fv - \hat{f}w + F_\lambda \quad (2.3a)$$

$$\frac{Dv}{Dt} - \frac{u^2 \tan \phi}{r} + \frac{vw}{r} = -\frac{1}{\rho r} \frac{\partial p}{\partial \phi} - fu + F_\phi \quad (2.3b)$$

$$\frac{Dw}{Dt} - \frac{u^2 + v^2}{r} = -\frac{1}{\rho} \frac{\partial p}{\partial z} - g + \hat{f}u + F_z \quad (2.3c)$$

where $\mathbf{u} = (u, v, w)$ is the fluid's velocity along the λ, ϕ, z directions

$$u = a \cos \phi \frac{\partial \lambda}{\partial t} \quad (2.4a)$$

$$v = a \frac{\partial \phi}{\partial t} \quad (2.4b)$$

$$w = \frac{\partial z}{\partial t} \quad (2.4c)$$

and the advective derivative (Equation 2.1) in spherical coordinates reads:

$$\frac{D}{Dt} = \frac{\partial}{\partial t} + \frac{u}{a \cos \phi} \frac{\partial}{\partial \lambda} + \frac{v}{a} \frac{\partial}{\partial \phi} + w \frac{\partial}{\partial z}. \quad (2.5)$$

Because a is the Earth's mean radius, z is height above the Earth's surface, and $r = a + z$, it follows that for the atmospheric heights under consideration, $z \ll a$ and r generally can be replaced by a . This is known as the *shallowness approximation*, because it results from the relatively shallow depth of the atmosphere compared to the Earth's radius. Also, since in climate-oriented general circulation models the motions of primary interest have characteristic horizontal space scales of hundreds to thousands of km and velocities on the order of 10 m s^{-1} , we can simplify Equation 2.3 further by eliminating several of the generally less-significant terms, such as $\hat{f}w$, $\hat{f}u$ and $\frac{u^2+v^2}{r}$ by assuming g is constant. In this approximations Equation 2.3 simplifies to (Washington and Parkinson, 2005):

$$\frac{Du}{Dt} - v \left(f + \frac{u \tan \phi}{a} \right) = -\frac{1}{a \cos \phi} \frac{1}{\rho} \frac{\partial p}{\partial \lambda} + F_\lambda \quad (2.6a)$$

$$\frac{Dv}{Dt} + u \left(f + \frac{u \tan \phi}{a} \right) = -\frac{1}{a} \frac{1}{\rho} \frac{\partial p}{\partial \phi} + F_\phi \quad (2.6b)$$

$$\frac{Dw}{Dt} = -\frac{1}{\rho} \frac{\partial p}{\partial z} - g + F_z. \quad (2.6c)$$

The second term on the left-hand side of Equation 2.6a represents the Coriolis force and the centrifugal force in the rotating reference frame of the Earth. f is the Coriolis parameter, which depends on the latitude ϕ and is given by $f = 2\Omega \sin \phi$. The Coriolis force is proportional to the velocity and acts perpendicular to the motion of the fluid, deflecting the fluid in different directions depending on the hemisphere. Note that the Coriolis term arises due to the rotation of the Earth, which introduces an apparent force in a rotating reference frame. This term depends explicitly on the latitude because of how the Earth's rotation affects the direction and magnitude of the Coriolis effect at different points on the Earth's surface. The Coriolis force explicitly depends on the sine of the latitude, as the projection of Ω onto the local horizontal plane is $\Omega \sin \phi$ (the latitude ϕ determines the angle between the Earth's rotational axis and the local vertical). Ω is the angular velocity vector of Earth's rotation, it points along the axis of rotation (towards the North Pole). At the Equator $\phi = 0$ the Coriolis effect is perpendicular to Ω and has a max horizontal effect. At the poles ($\phi = \pm 90$) the effect aligns with Ω , and only the vertical motion is affected.

On the right side of all the three equations 2.6 we find the pressure gradient force in the longitudinal (first) and latitudinal (second) directions, which drives fluid motion due to differences in pressure. The terms F_λ , F_ϕ and F_z represent an *additional force* term that could represent any other forcing acting on the fluid parcel in the longitudinal, latitudinal and vertical direction. It might include friction, external forces, or any other model-specific forces not accounted for in the other terms.

The term $\frac{u \tan \phi}{a}$ present in Equation 2.6a accounts for the centrifugal force resulting from the Earth's rotation. Here, u is the east-west velocity, ϕ is the latitude, and a is the Earth's radius. The centrifugal force is stronger near the equator, and this term adjusts the Coriolis effect to account for that. $\frac{\partial p}{\partial \lambda}$ indicates how pressure changes as you move longitudinally, i.e. east or west. The term $a \cos \phi$ accounts for the spherical geometry of the Earth and the fact that distances between lines of longitude vary with latitude (they are widest at the Equator and shrink towards the poles). This term describes the acceleration due to the horizontal pressure gradient in the longitudinal direction, with the pressure gradient force causing flow from regions of higher to lower pressure.

The term $\frac{v \tan \phi}{a}$ in Equation 2.6b is the centrifugal force term in the north-south direction, considering Earth's curvature. $\frac{p}{\phi}$ represents the pressure gradient in the latitude direction, and it drives motion from high to low pressure.

As for the vertical direction, Equation 2.6c, the the vertical component of the Coriolis force is negligible because Ω is nearly parallel to the vertical axis in most regions. In rotating systems like the atmosphere or oceans, vertical Coriolis terms are often ignored. Gravity acts downward and opposes the upward motion.

The system of equations ?? is not closed: there are 5 variables but only 3 equations. Therefore additional relationships need to be found to close the system. As we shall now see, the fundamental conservation laws allow to do that.

2.2.2 Mass conservation

The mass of the fluid must be conserved locally, because there are now sinks or sources in the atmosphere itself, so we want to write the mass of a volume of atmosphere fixed in space as

$$M = \int_V \rho dV$$

the mass in the volume can only change if there is a flux of mass at surface S ,

$$\frac{\partial}{\partial t} \int_V \rho dV = - \int_S \rho \mathbf{u} \cdot \mathbf{n} dS$$

using the divergence theorem however we have

$$\frac{\partial}{\partial t} \int_V \rho dV = - \int_V \nabla \cdot (\rho \mathbf{u}) dV$$

because the volume is not changing with time we can bring the derivative inside the integral and we get

$$\int_V \frac{\partial \rho}{\partial t} + \nabla \cdot (\rho \mathbf{u}) dV = 0$$

but the volume is arbitrary, so it must be that

$$\frac{\partial \rho}{\partial t} + \nabla \cdot (\rho \mathbf{u}) = 0 \quad (2.7)$$

is valid locally.

The **conservation of mass** or **continuity equation** 2.7 ensures that the mass is conserved in the system expresses how the density of air or water changes over time due to processes like flow and diffusion. In particular, $\nabla \cdot (\rho \mathbf{v})$ represents the divergence of the mass flux, which accounts for the movement of the mass.

2.2.3 First law of thermodynamics

We have still at our disposal the conservation of thermodynamical energy and so we can also use the first law of thermodynamics for a gas, that is a statement of internal energy, where c_v is the specific heat for air at constant volume and T is the temperature in Kelvins:

$$c_v \frac{DT}{Dt} = -p \frac{D}{Dt} \left(\frac{1}{\rho} \right) + Q \quad (2.8)$$

where we included the temperature and heating/cooling term Q (which is the net heat gain or loss to the external sources, for example the solar insolation, heating or cooling due to long wave radiation, latent heating due to condensation of water vapor into liquid water, and sensible heating due to conduction and convection). The state variables are then linked by the **equation of state** for an ideal gas

$$p = \rho RT \quad (2.9)$$

where R is the gas constant for dry air.

We can now use 2.9 to write the energy equation 2.8 (or the temperature equation) in a different form,

$$c_v \frac{DT}{Dt} = -p \frac{D}{Dt} \left(\frac{RT}{p} \right) + Q = -R \frac{DT}{Dt} + \frac{RT}{p} \frac{Dp}{Dt} + Q$$

or (since for an ideal gas $c_p = c_v + R$),

$$c_p \frac{DT}{Dt} - \frac{1}{\rho} \frac{Dp}{Dt} = Q$$

For many purpose atmospheric and oceanic motions can be considered essentially adiabatic. However, for climate studies, the assumption of exclusively adiabatic processes is not appropriate since the amount of heat added or lost to a unit volume of air or water over a long period of time can be substantial. For adiabatic processes $Q = 0$:

$$\begin{aligned} c_p \frac{DT}{Dt} - \frac{1}{\rho} \frac{Dp}{Dt} &= 0 \\ \frac{c_p}{T} \frac{DT}{Dt} - \frac{R}{p} \frac{Dp}{Dt} &= 0 \\ \frac{D}{Dt} \log T - \frac{R}{c_p} \frac{D}{Dt} \log p &= 0 \end{aligned}$$

integrating it we get

$$\log T/T_0 - \log \left(\frac{p}{p_0} \right)^{R/c_p} = \text{const}$$

or

$$\frac{T}{T_0} \left(\frac{p_0}{p} \right)^{R/c_p} = \text{const} \quad (2.10)$$

so the quantity, known as *potential temperature*

$$\theta = T \left(\frac{p_0}{p} \right)^{R/c_p} \quad (2.11)$$

is conserved in adiabatic processes and the thermodynamics equation can be written as

$$\frac{D\theta}{Dt} = Q. \quad (2.12)$$

Equation 2.12 quantifies the rate of change of a scalar quantity (like temperature or moisture) for a fluid parcel moving through space. The source term Q could represent a source of energy or mass, such as heat from the sun or moisture added by evaporation. In the context of a weather or climate model, this would represent how temperature (or another variable) changes as the air parcel moves and as energy is gained or lost.

2.2.4 Hydrostatic balance

Under the action of gravity the vertical component of the pressure gradient force balances the action of gravity, resulting in very small vertical acceleration

$$\frac{\partial p}{\partial z} = -g\rho$$

then if we take the vertical derivative of Equation 2.10

$$\frac{1}{T_0} \frac{dT}{dz} \left(\frac{p_0}{p} \right)^{R/c_p} - \frac{p_0}{p^2} \frac{R}{c_p} \frac{T}{T_0} \left(\frac{p_0}{p} \right)^{R/c_p-1} \frac{dp}{dz} = 0$$

simplifying

$$\frac{dT}{dz} - \frac{p_0}{p^2} \frac{R}{c_p} T \left(\frac{p_0}{p} \right)^{-1} \frac{dp}{dz} = 0$$

or

$$\frac{dT}{dz} - \frac{1}{p} \frac{R}{c_p} T \frac{dp}{dz} = \frac{dT}{dz} + g\rho \frac{1}{p} \frac{R}{c_p} T = 0$$

but using the equation of state 2.9

$$\frac{dT}{dz} = -\frac{g}{c_p} \quad (2.13)$$

yields the temperature gradient with height under adiabatic conditions and when the hydrostatic balance is valid. This is known as the *adiabatic lapse rate*; for sea-level dry air at 0°C $c_p \simeq 1000 \text{ J kg}^{-1} \text{ K}^{-1}$, thus we get an estimate of it

$$\frac{g}{c_p} = 10^\circ\text{C km}^{-1}. \quad (2.14)$$

Under this assumptions there is a linear drop in temperature with height.

If we integrate over height z , assuming isothermal atmosphere, we get an exponential density ρ and pressure p decay with height:

$$p(z) = p_0 \exp \left(-\frac{RT}{g} z \right). \quad (2.15)$$

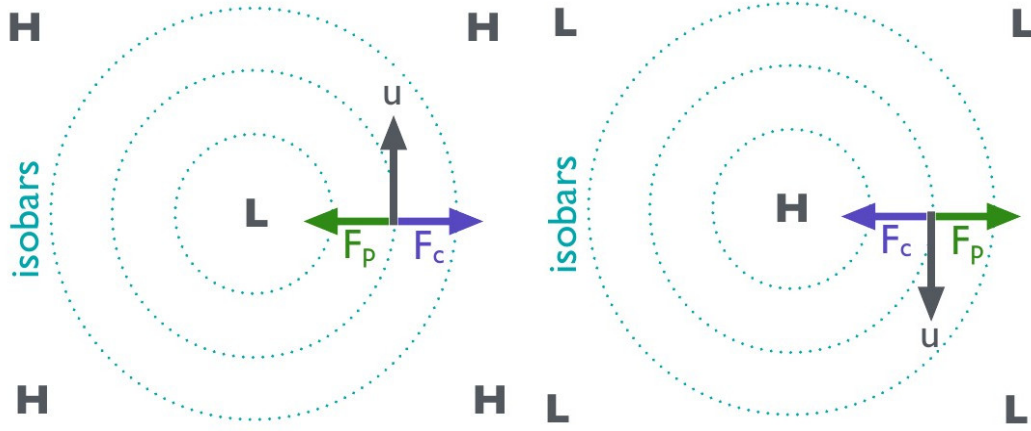


Figure 2.2: Geostrophic winds follow a counterclockwise path in the Northern Hemisphere (and a clockwise path in the Southern Hemisphere) along the isobars of low pressure cells (cyclones). Geostrophic winds follow a clockwise path in the Northern Hemisphere (and a counterclockwise path in the Southern Hemisphere) along the isobars of high pressure cells (anti-cyclones). Taken from [INTEGRATE Teaching Package](#).

2.2.5 Geostrophic balance

Geostrophic balance is the balance between Coriolis Force and the horizontal component of the pressure gradient force. Under this assumptions, equations 2.6a and 2.6b become, respectively (Gill, 1982):

$$fv = \frac{1}{\rho} \frac{\partial p}{\partial x} \quad (2.16)$$

$$fu = -\frac{1}{\rho} \frac{\partial p}{\partial y} \frac{df}{dx} \quad (2.17)$$

The pressure gradient force (PGF) pushes air or water from high pressure to low pressure. The Coriolis force deflects the motion to the right in the Northern Hemisphere and to the left in the Southern Hemisphere. In geostrophic balance, these forces are equal in magnitude and opposite in direction. The geostrophic balance assumes the flow is steady and does not accelerate, so it neglects the effects of inertia. This balance is most accurate for large-scale motions (e.g., planetary or synoptic scales) where friction and other forces are negligible. Vertical motions are typically much smaller than horizontal motions and are neglected in geostrophic balance.

$$\mathbf{v} = \hat{\mathbf{k}} \times \frac{1}{f\rho} \nabla p \quad (2.18)$$

In geostrophic balance:

- Air or water flows parallel to the isobars (lines of constant pressure) or contours of constant geopotential height.
- The speed of the geostrophic flow increases with stronger pressure gradients (closer isobars).

However, on small scales (e.g., tornadoes, boundary layers), friction and other forces become important, so geostrophic balance is less accurate. Near the Equator, The Coriolis parameter (f) approaches zero, making the geostrophic balance invalid.

Coriolis Factors

The Coriolis forces derives from the conservation of angular momentum.

$$\frac{D}{Dt} (R_A(\Omega R_A + u)) = 0$$

or

$$2\Omega R_A \frac{dR_A}{dt} + u \frac{dR_A}{dt} + R_A \frac{Du}{Dt} = 0$$

rearraging

$$\frac{Du}{Dt} = (2\Omega R_A + u) \frac{dR_A}{dt}$$

The Coriolis components then are $2\Omega \sin \phi$ and $2\Omega \cos \phi$. For the horizontal and vertical

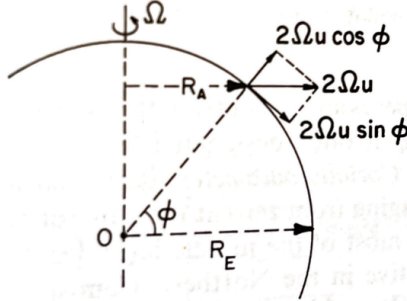


Figure 2.3: Coriolis factors

components respectively: $f = 2\Omega \sin \phi$.

2.2.6 The full set of governing equations for the atmosphere

The full set of governing equations (Equations 2.6, 2.12, 2.7 and 2.9) under the approximations described in Section 2.2.1 (shallowness condition, neglect of w terms) can now be written as¹:

$$\frac{Du}{Dt} - v \left(f + \frac{u \tan \phi}{a} \right) = -\frac{1}{a \cos \phi} \frac{1}{\rho} \frac{\partial p}{\partial \lambda} + F_\lambda \quad (2.19a)$$

$$\frac{Dv}{Dt} + u \left(f + \frac{u \tan \phi}{a} \right) = -\frac{1}{a} \frac{1}{\rho} \frac{\partial p}{\partial \phi} + F_\phi \quad (2.19b)$$

$$\frac{Dw}{Dt} = -\frac{1}{\rho} \frac{\partial p}{\partial z} - g + F_z \quad (2.19c)$$

$$\frac{D\theta}{Dt} = Q \quad (2.19d)$$

$$\frac{\partial \rho}{\partial t} + \frac{1}{a \cos \phi} \left[\frac{\partial}{\partial \lambda} (\rho u) + \frac{\partial}{\partial \phi} (rv \cos \phi) \right] + \frac{\partial}{\partial z} (\rho w) = 0 \quad (2.19e)$$

$$p = \rho RT \quad (2.19f)$$

where we have expanded the divergence in spherical coordinates (see Appendix A.1.2.).

These equations are still not closed because we will need to express the heating/cooling term Q and the friction terms F as a function of the state variables. This will require a theory of the processes that drive them. Where $R = 287 \text{ J kg}^{-1} \text{ K}^{-1}$ is the gas constant for dry air and $c_p \simeq 1.005 \text{ J g}^{-1} \text{ K}^{-1}$ is the specific heat at constant pressure, $c_v = 0.718 \text{ J g}^{-1} \text{ K}^{-1}$ is the specific heat at constant volume, $\kappa = \frac{R}{c_p}$ and $\gamma = c_p/c_v$ is their ratio.

¹The hydrostatic condition is not enforced for the system 2.19.

2.2.7 β -plane approximation

It can be convenient to shift the coordinate system when the latitudinal extent of motion is small relative to motion parameters expressed in adimensional numbers. In such cases, a tangent coordinate system is applied at a specific latitude ϕ_0 , resulting in a Cartesian β -plane with zonal and meridional coordinates (x, y) .

On the β -plane, the planetary vorticity (see Equation ??) f is linearized as $f = f_0 + \beta y$, where $\beta = \frac{\partial f}{\partial y}(\phi_0)$. The northward displacement $y = a(\phi - \phi_0)$ represents deviation from the reference latitude.

This approximation simplifies geophysical fluid dynamics equations by neglecting rotation, sphericity, and certain meridional coordinates. The equations 2.19 projected onto the β -plane simplify to

$$\frac{Du}{Dt} - fv = -\frac{1}{\rho} \frac{\partial p}{\partial x} + F_x \quad (2.20)$$

$$\frac{Dv}{Dt} + fu = -\frac{1}{\rho} \frac{\partial p}{\partial y} + F_y \quad (2.21)$$

$$\frac{Dw}{Dt} = -\frac{1}{\rho} \frac{\partial p}{\partial z} - g + F_z \quad (2.22)$$

$$\frac{D\theta}{Dt} = Q \quad (2.23)$$

$$\frac{\partial \rho}{\partial t} + \nabla \cdot (\rho \mathbf{u}) = 0 \quad (2.24)$$

$$p = \rho RT. \quad (2.25)$$

2.3 Linear solutions to the primitive equations

We look for solution that describe small oscillation away from a basic state, in this case assumed in hydrostatic balance with constant wind of velocity u , and I'm looking at deviation from this basic state:

$$\frac{\partial p_0}{\partial z} = -g\rho_0 = -\frac{gp_0}{RT_0} \quad (2.26)$$

With the further assumption of isotherm atmosphere we can integrate to get:

$$p_0(z) = p_R \exp(-z/H) \quad (2.27)$$

and $H = \frac{RT_0}{g}$ is the scale height.

As we have seen, the primitive equations are a system of nonlinear partial differential equations governing fluid motion on a rotating sphere. These include momentum equations, continuity (mass conservation), thermodynamic equations and the equation of state. Since solving the full nonlinear system is often impractical, the system is linearized to analyze small deviations (or perturbations) from a reference state (steady flow or a state of rest). Assume the flow can be separated into a basic state and a perturbation:

$$\begin{aligned} u &= u_0 + u' \\ v &= v_0 + v' \\ \theta &= \theta_0 + \theta' \\ p &= p_0 + p' \end{aligned}$$

The resulting linearized primitive equations describe how perturbations evolve over time and space (linear equations are obtained for the prime variables neglecting all terms quadratic in

perturbation). For instance, the pressure gradient becomes:

$$\frac{1}{\rho_0 + \rho'} \nabla(p_0 + p') + g\hat{\mathbf{k}} \approx \frac{1}{\rho_0 + \rho'} \nabla p' + g\hat{\mathbf{k}} = \frac{1}{\rho_0} \frac{1}{1 + \frac{\rho'}{\rho_0}} \nabla p' + g\hat{\mathbf{k}} = \frac{1}{\rho_0} \nabla p' + g\hat{\mathbf{k}} \quad (2.28)$$

and the potential temperature:

$$\theta = T \left(\frac{p_R}{p} \right)^k = \frac{p_R^k}{R} \frac{p^{1-k}}{\rho} \approx \theta_0 \left[1 + \frac{1}{\gamma} \left(\frac{p'}{p_0} \right) - \frac{\rho'}{\rho_0} \right]$$

hence,

$$\frac{\theta'}{\theta_0} = \frac{1}{\gamma} \frac{p'}{p_0} - \frac{\rho'}{\rho_0} \quad (2.29)$$

with $\gamma = \frac{c_p}{c_v}$, $k = \frac{R}{c_v}$, $R = c_p - c_v$.

2.3.1 Waves

The linearized system often supports wave-like solutions. These solutions arise naturally due to the restoring forces in the equations, such as:

- Pressure gradient drives the oscillations through compressibility or buoyancy
- Coriolis force introduces rotational effects leading to inertial and planetary waves
- Gravity acts as a restoring force for vertical displacement, driving internal gravity waves.

We take the equations for perturbation:

$$\begin{aligned} \frac{\partial u}{\partial t} + U \frac{\partial u}{\partial x} + \frac{1}{\rho_0} \frac{\partial p}{\partial x} &= 0 \\ \frac{\partial w}{\partial t} + U \frac{\partial w}{\partial x} + \frac{1}{\rho_0} \frac{\partial p}{\partial z} + g \frac{\rho}{\rho_0} &= 0 \\ \frac{\partial \rho}{\partial t} + U \frac{\partial \rho}{\partial x} + w \frac{\partial \rho_0}{\partial z} + \rho_0 \left(\frac{\partial u}{\partial x} + \frac{\partial w}{\partial z} \right) &= 0 \\ \frac{\partial \theta}{\partial t} + U \frac{\partial \theta}{\partial x} + w \frac{\partial \theta_0}{\partial z} &= 0 \\ \frac{\theta}{\theta_0} + \frac{\rho}{\rho_0} + \frac{1}{\gamma} \frac{p}{p_0} &= 0 \end{aligned}$$

Basically to find solutions, assume the perturbations take the form of plane waves:

$$\mathbf{u}'(x, t) = \hat{\mathbf{u}} e^{i(\mathbf{k} \cdot \mathbf{x} - \omega t)}$$

where $\hat{\mathbf{u}}$ is the amplitude of the perturbation, \mathbf{k} is the wavevector, ω the angular velocity. Substituting this kind of wave into the linearized equations leads to a dispersion relation, which relates ω to \mathbf{k} and the physical parameters of the system (Coriolis, ...). The perturbation equations link the restoring forces to wave properties:

1. The momentum equations describe how velocity perturbations interact with pressure gradients and Coriolis forces.
2. The continuity equation ensures mass conservation, connecting velocity and density perturbations.
3. The thermodynamic equation relates temperature, pressure and density perturbations

Imposing the hydrostatic approximation from the beginning would mean putting to zero from the start the time derivative of w in the momentum equation in the vertical. This basically is equivalent to say that we are removing the explicit dependence of the vertical velocity on time and therefore we will get waves similar to the Boussinesq approximation. The hydrostatic approximation eliminates vertical propagating sound waves, but the Lamb waves still exists.

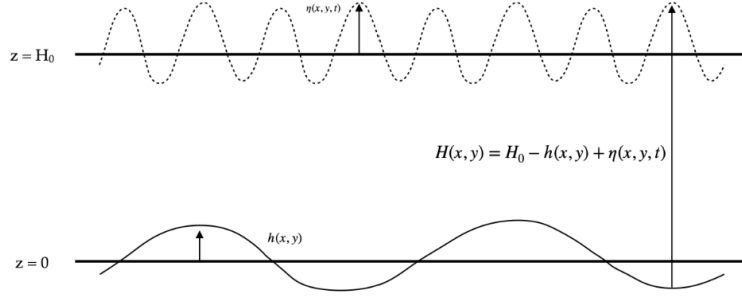


Figure 2.4: Homogeneous flow

2.4 Homogeneous flows

The motion of the atmosphere is most appropriately described by three-dimensional equations that describes the horizontal and vertical motion of the fluid, however a lot can be understood by considering a simpler system that consider the motion of a free surface of a inviscid, homogeneous and incompressible fluid. These equations are variously referred to as one-level primitive equations or the *shallow water equations*.

The system is described in Figure 2.4, it is an homogenous layer of fluid covering the entire spherical planet. We have included a bottom topography $h(x, y)$ and a deformation of the free surface $\eta(x, y)$. The convention is such positive deformation of the surface are increasing the depth of the fluid, whereas positive deformation of the bottom are decreasing it.

We have introduced here cartesian coordinates (x, y) such that $dx \approx a \cos \theta d\lambda$ and $dy \approx a d\theta$, we will also define $f = 2\Omega \sin \theta$, then the incompressible equations of motion can be written as

$$\begin{aligned}\frac{\partial u}{\partial t} &= -u \frac{\partial u}{\partial x} - v \frac{\partial u}{\partial y} + fv - \frac{1}{\rho} \frac{\partial p}{\partial x} \\ \frac{\partial v}{\partial t} &= -u \frac{\partial v}{\partial x} - v \frac{\partial v}{\partial y} - fu - \frac{1}{\rho} \frac{\partial p}{\partial y} \\ \frac{\partial w}{\partial t} &= -u \frac{\partial w}{\partial x} - v \frac{\partial w}{\partial y} + g - \frac{1}{\rho} \frac{\partial p}{\partial z} \\ \frac{\partial u}{\partial x} + \frac{\partial v}{\partial y} + \frac{\partial w}{\partial z} &= 0\end{aligned}$$

If the aspect ratio $\delta \approx H/L$ is small then hydrostatic balance is maintained to order δ^2 and so

$$\frac{\partial p}{\partial z} = -\rho g + O(\delta^2)$$

because the density is constant we can integrate it from 0 to z and get

$$p = -\rho g(H_0 + \eta - z) + p_0$$

where we have used the boundary condition at the top $p(x, y, H_0 + \eta) = p_0$. The horizontal pressure gradients are independent of z

$$\begin{aligned}\frac{\partial p}{\partial x} &= \rho g \frac{\partial \eta}{\partial x} \\ \frac{\partial p}{\partial y} &= \rho g \frac{\partial \eta}{\partial y}\end{aligned}$$

because the horizontal accelerations are independent of z , than also the velocities are independent of z , if they are so at the beginning. This is in fact a consequence of the Taylor-Proudman theorem applied to a homogeneous fluid. We can then write the horizontal momentum equations

$$\begin{aligned}\frac{\partial u}{\partial t} &= -u \frac{\partial u}{\partial x} - v \frac{\partial u}{\partial y} + fv - g \frac{\partial \eta}{\partial x} \\ \frac{\partial v}{\partial t} &= -u \frac{\partial v}{\partial x} - v \frac{\partial v}{\partial y} - fu - g \frac{\partial \eta}{\partial y}\end{aligned}$$

Because u and v are independent of z allows us to integrate vertically the divergence equation from the surface $h(x, y)$ to an height z

$$w(x, y, z, t) = -z \left(\frac{\partial u}{\partial x} + \frac{\partial v}{\partial y} \right) + \omega(x, y, t)$$

The kinematic condition for the bottom can be written as

$$\frac{D}{Dt}(z - h) = 0$$

or

$$w(x, y, h, t) = u \frac{\partial h}{\partial x} + v \frac{\partial h}{\partial y}$$

so the function ω is

$$\omega(x, y, t) = u \frac{\partial h}{\partial x} + v \frac{\partial h}{\partial y} + h \left(\frac{\partial u}{\partial x} + \frac{\partial v}{\partial y} \right)$$

then the vertical velocity can be written as

$$w(x, y, z, t) = (h - z) \left(\frac{\partial u}{\partial x} + \frac{\partial v}{\partial y} \right) + u \frac{\partial h}{\partial x} + v \frac{\partial h}{\partial y}$$

Using now the kinematic boundary condition at the top ($z = H_0 + \eta$)

$$w(x, y, H_0 + \eta, t) = \left(\frac{\partial}{\partial t} + u \frac{\partial}{\partial x} + v \frac{\partial}{\partial y} \right) (H_0 + \eta)$$

combining the last two equation we get an equation for the height

$$\frac{\partial \eta}{\partial t} + \frac{\partial}{\partial x} (H_0 + \eta - h)u + \frac{\partial}{\partial y} (H_0 + \eta - h)v = 0$$

and so we can now write the complete equations, introducing the total depth of the fluid $H = H_0 + \eta - h$:

$$\begin{aligned}\frac{\partial u}{\partial t} &= -u \frac{\partial u}{\partial x} - v \frac{\partial u}{\partial y} + fv - g \frac{\partial H}{\partial x} \\ \frac{\partial v}{\partial t} &= -u \frac{\partial v}{\partial x} - v \frac{\partial v}{\partial y} - fu - g \frac{\partial H}{\partial y} \\ \frac{\partial H}{\partial t} &= -\frac{\partial(uH)}{\partial x} - \frac{\partial(vH)}{\partial y}\end{aligned}$$

Linearizing around a state of rest, constant rotation:

$$\begin{aligned}\frac{\partial u}{\partial t} - fv &= -g \frac{\partial \eta}{\partial x} \\ \frac{\partial v}{\partial t} + fv &= -g \frac{\partial \eta}{\partial y} \\ \frac{\partial \eta}{\partial t} &= -H_0 \left(\frac{\partial u}{\partial x} + \frac{\partial v}{\partial y} \right)\end{aligned}$$

the solutions are, respectively:

$$\begin{aligned}u(x, y, t) &= \operatorname{Re} \left[\tilde{u} \sin(l y) e^{i(kx - \omega t)} \right] \\ v(x, y, t) &= \operatorname{Re} \left[\tilde{v} \sin(l y) e^{i(kx - \omega t)} \right] \\ \eta(x, y, t) &= \operatorname{Re} \left[\tilde{\eta} \sin(l y) e^{i(kx - \omega t)} \right]\end{aligned}$$

two modes², a stationary mode and a gravity mode (Poincare' modes): $\omega = 0$ and $\omega^2 = f^2 + gH_0(k^2 + l^2)$

2.4.1 The vorticity equation on the β -plane

The spherical geometry maybe cumbersome without adding much the conceptual discussions, so it may be convenient to introduce Cartesian coordinates (x, y) such that $dx \approx a \cos \theta d\lambda$ and $dy \approx ad\theta$, we will also define $f = 2\Omega \sin \theta$, then we obtain equation formally identical to the Cartesian equation described previously

$$\begin{aligned}\frac{\partial u}{\partial t} &= -u \frac{\partial u}{\partial x} - v \frac{\partial u}{\partial y} + fv - g \frac{\partial \eta}{\partial x} \\ \frac{\partial v}{\partial t} &= -u \frac{\partial v}{\partial x} - v \frac{\partial v}{\partial y} - fu - g \frac{\partial \eta}{\partial y} \\ \frac{\partial u}{\partial x} + \frac{\partial v}{\partial y} &= 0\end{aligned}$$

where we have kept the pressure terms, though they are zero in this case (h is a constant) as a placeholder. In vector notation (all vectors are two-dimensional)

$$\frac{\partial \mathbf{u}}{\partial t} = -(\mathbf{u} \cdot \nabla) \mathbf{u} - f(\hat{\mathbf{k}} \times \mathbf{u}) - \nabla \eta$$

using the vector identity³

$$\frac{1}{2} \nabla(\mathbf{u} \cdot \mathbf{u}) = (\mathbf{u} \cdot \nabla) \mathbf{u} + \mathbf{u} \times (\nabla \times \mathbf{u})$$

so substituting in the equation

$$\frac{\partial \mathbf{u}}{\partial t} = -(\zeta + f) \hat{\mathbf{k}} \times \mathbf{u} - \nabla \left(\eta + \frac{1}{2} |\mathbf{u}|^2 \right) \quad (2.30)$$

(for 2-dimensional flows $\nabla \times \mathbf{u} = \zeta \hat{\mathbf{k}}$).

and to express more clearly the components

²mode in this context refers to a specific solution or pattern of motion that satisfies the governing equations of the flow, under certain boundaries or initial conditions.

³For a general vector \mathbf{A} :

$$\frac{1}{2} \nabla(A \cdot A) = (A \cdot \nabla) A + A \times (\nabla \times A)$$

$$\begin{aligned}\frac{\partial u}{\partial t} &= (\zeta + f)v - \frac{\partial}{\partial x}(\eta + \frac{1}{2}|\mathbf{u}^2|) \\ \frac{\partial v}{\partial t} &= -(\zeta + f)u - \frac{\partial}{\partial y}(\eta + \frac{1}{2}|\mathbf{u}^2|)\end{aligned}$$

By taking the curl of eq.2.30 we obtain an equation for the vorticity (as it will be discussed in Sec.??):

$$\begin{aligned}\frac{\partial \zeta}{\partial t} &= -\frac{\partial}{\partial x}(\zeta + f)u - \frac{\partial}{\partial y}(\zeta + f)v \\ &\quad - \frac{\partial}{\partial x} \frac{\partial}{\partial y}(p + \frac{1}{2}|\mathbf{u}^2|) + \frac{\partial}{\partial y} \frac{\partial}{\partial x}(p + \frac{1}{2}|\mathbf{u}^2|) \\ &= -\frac{\partial}{\partial x}(\zeta + f)u - \frac{\partial}{\partial y}(\zeta + f)v = -\mathbf{u} \cdot \nabla(\zeta + f)\end{aligned}$$

where we have used the non divergence condition $\frac{\partial u}{\partial x} + \frac{\partial v}{\partial y} = 0$ in the last step. Once again, this is the equation for the conservation of total vorticity where we can see that the relative vorticity is a sort of additional Coriolis effect (or alternatively that the Coriolis term is a source of vorticity). Because of the β -plane $f = f_0 + \beta y$:

$$\frac{\partial \zeta}{\partial t} = -u \frac{\partial \zeta}{\partial x} - v \frac{\partial \zeta}{\partial y} - \beta v \quad (2.31)$$

that is the non-divergent barotropic vorticity equation. And the potential vorticity:

$$\frac{D}{Dt}(\zeta + f) = 0 \quad (2.32)$$

$f = 2\Omega \sin(\theta)$ is the Coriolis coefficient, that is the vertical component of the Earth planetary vorticity.

In the new coordinates (x, y) for longitude and latitude, the streamfunction and the vorticity then are

$$u = -\frac{\partial \psi}{\partial y} \quad v = \frac{\partial \psi}{\partial x} \quad \zeta = \frac{\partial x}{\partial x} - \frac{\partial u}{\partial y} = \nabla^2 \psi$$

introducing the Jacobian operator

$$J(A, B) = \frac{\partial A}{\partial x} \frac{\partial B}{\partial y} - \frac{\partial A}{\partial y} \frac{\partial B}{\partial x}$$

we obtain a single equation for the streamfunction

$$\frac{\partial}{\partial t} \nabla^2 \psi + J(\psi, \nabla^2 \psi + f_0 + \beta y) = 0$$

that represents the quasi-geostrophic potential vorticity. Vorticity is a vertical component of the velocity, and appears coupled with f , where f is a property of the Earth and ζ is a property of the flow. Because the potential vorticity is conserved with the flow, if you have something at rest at the Equator and you move it Poleward, it acquire vorticity and starts speeding .

2.5 Rossby waves

Rossby waves or planetary waves are large-scale waves that arise in a rotating fluid, such as the Earth's atmosphere or oceans, due to the variation of the Coriolis parameter f with latitude. In particular, they are caused by the β -effect, i.e. $\beta = \frac{\partial f}{\partial y} = \frac{2\Omega \cos \phi}{a}$. These waves typically have very large horizontal wavelengths and govern large-scale motions in the atmosphere and

oceans, their restoring force is the variation of the Coriolis force with latitude. Rossby waves are much slower than other atmospheric or oceanic waves, such as gravity or sound waves.

Linearizing around a basic state U :

$$\frac{\partial \zeta'}{\partial t} + U \frac{\partial \zeta'}{\partial x} - \beta \nu' = 0 \quad (2.33)$$

the solutions are:

$$\psi(x, y, t) = \text{Re} \left[\tilde{\psi} \sin(l y) e^{i(kx - \omega t)} \right] \quad (2.34)$$

as⁴

$$\zeta = \nabla^2 \psi = -(k^2 + l^2) \psi$$

with $u = -il\psi$ and $\nu = ik\psi$ the dispersion relation is

$$\omega = U k - \frac{k\beta}{(k^2 + l^2)}$$

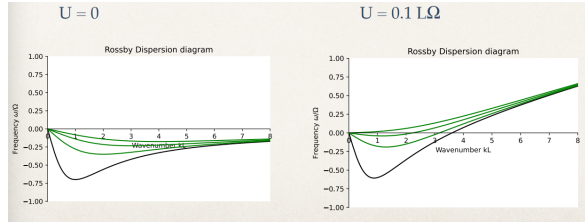


Figure 2.5: Rossby waves

2.6 Fundamental processes

Different climate models incorporate all the complex physical processes occurring in the climate system using a variety of methods. The dynamic involves interactions between motions, thermodynamics, and atmospheric water content.

2.6.1 Radiation

The radiation that heats and cools the climate system can be divided into two parts: solar radiation (shortwave) and terrestrial radiation (longwave). All gases emit and absorb radiation, and each chemical element or combination of elements has a distinct spectrum indicating at which electromagnetic wavelengths its emissions occur. In some cases, the emission may be confined to narrow portions of the electromagnetic spectrum rather than being a smoothly varying function of wavelength. This phenomenon of distinct, discrete emission spectra results from the emission of radiation as an electron moves from one orbit around an atomic nucleus to another orbit closer to the nucleus. If the atom is excited by absorbing energy, then the electron can go to a higher (outer) discrete orbit. As electrons return to the inner orbits, emission occurs in the ultraviolet part of the spectrum, producing the emission spectra. If electrons return to intermediate orbits instead of higher orbits, the emission is in the visible part of the spectrum; for the outer orbits, the emission is in the infrared. So far we have discussed only the emission of energy from a gas, not the absorption of energy. Suppose radiational energy enters an atomic or molecular gas and is absorbed. In that case, it can increase the atomic or molecular energy levels by the same amount of energy involved in the emission. This absorption can be just as discrete or selective as the emission. Thus, if radiation entering

⁴This will be understood after a reading of the Spectral Transformation method in sec.??.

a gas cannot excite the atoms or molecules in any energy form, then the radiational energy will not be absorbed or emitted in the gas.

In the Earth's atmosphere, ozone, carbon dioxide, and water vapor are very important triatomic molecules that both emit and absorb radiation in certain parts of the electromagnetic spectrum that affect the climate system.

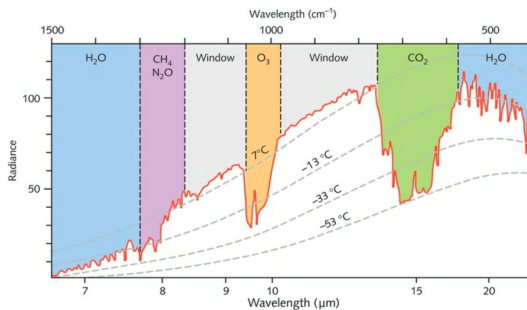


Figure 2.6: Earth's spectrum

As we can see in figure 2.6 ozone is a very strong absorber in the 9-10 μm region, carbon dioxide has absorption maxima in the 2, 3, 4, and 13-17 μm regions, and water vapor has several absorption regions in the 1-8 μm range and at wavelengths greater than 13 μm .

The radiational heating and cooling computation in climate models is usually done by calculating upward and downward fluxes through unit horizontal areas, considering the vertical distributions of temperature, water vapor, and other radiative absorbing gases such as carbon dioxide and ozone.

The blackbody radiation curve was determined theoretically by Max Planck in 1900. A result of Planck's equation is the earlier displacement law of Wien, that the wavelength of maximum intensity $\frac{2897.8}{T}$ where T is the temperature of the blackbody. For the Earth, the approximate global mean surface temperature is 293 K, which yields a maximum intensity near $9.9\mu\text{m}$ whereas for the sun the surface temperature is approximately $T = 6110\text{K}$ which yields a maximum intensity at $0.474\mu\text{m}$. The overlap of the blackbody radiation curves for the Earth and for the sun's radiation reaching the Earth is not great, and consequently solar and terrestrial radiation can be separated based on wavelength.

Much of the fundamental physics governing radiation transfer is embodied in the following two laws:

- Lambert's law, which provides a formulation for the decrease in intensity of radiation of a given wavelength as the radiation passes through a given amount of absorbing gas

$$\frac{d}{dz}[I] = -Ik\rho$$

where k is the absorption coefficient (which tells us what kind of mass is present), ρ is the density of the layer, and I is the radiance, defined as the energy per unit time per unit area per unit solid angle $d\omega$

- Kirchhoff's law, states that there is a proportionality between radiative absorptivity and emissivity of a gas at the same temperature for any wavelength. A good absorber of radiation at some wavelength is also a good emitter of radiation at the same wavelength.

In particular, it is usually identified as *absorptivity* the ratio of the amount of radiative energy absorbed to the total incident radiation, and *emissivity* is the ratio of the emitted radiation to the maximum possible emitted radiation at the same temperature.

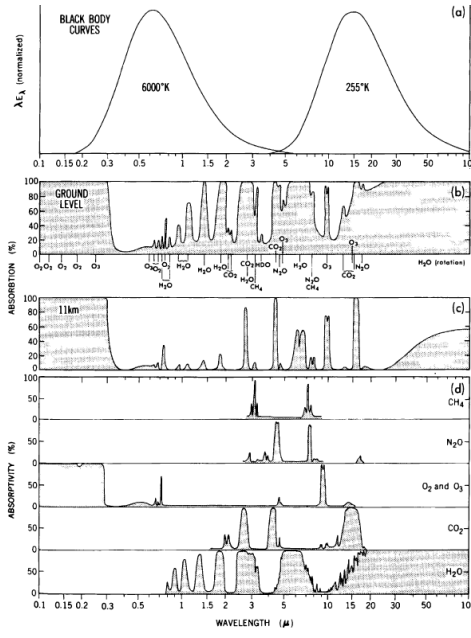
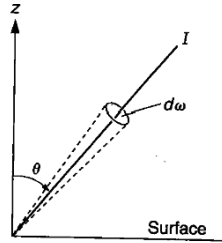


Figure 2.7: Black body curves for the solar radiation and the terrestrial radiation for the entire atmosphere and the first 11 km of the atmosphere

The 2.6.1 shows the relationship between intensity from some given direction, unit solid angle $d\omega$, and the surface, $R0.38$



such that integration over θ of the hemisphere above the horizontal surface yields the flux, F , arriving from all angles:

$$F = \int (I \cos \theta) d\omega \quad (2.35)$$

Dividing 2.35 by I and forming integrals over optical depth on either side yield

$$\int \frac{dI}{I} = - \int k\rho dz$$

which becomes

$$\ln \left(\frac{I}{I_0} \right) = - \int k\rho dz$$

upon integrating the left-hand side. This can be written exponentially as

$$I = I_0 e^{-\chi}$$

$$\chi = \int k\rho dz$$

where χ is the optical depth or optical path length (rate at which the radiance is degraded, if you move upward, at a certain point you get zero because you have traveled enough to absorb all the radiation) and

$$\tau = e^{-\chi}$$

is the frictional transmission, indicating the fraction of the original radiance that get transmitted to optical depth within attenuating gas. If $\chi = 1$, then $\tau = 0.37$, which means the initial intensity I is decreased by a factor of 0.63, for normal atmospheric conditions χ in typically much less than 1.

For a blackbody, the emission is also described by Lambert's law with a different sign

$$dI = B(T)k\rho dz \quad (2.36)$$

Integrating 2.36 over a hemisphere, the Stefan-Boltzmann law is then obtained

$$\int_0^{2\pi} B(T) \cos \theta d\omega = \sigma T^4$$

or

$$\pi B(T) = \sigma T^4$$

The change of radiance at a point z is made up of two fluxes

$$\frac{1}{\rho} \frac{dI}{dz} = -k(I - B(T))$$

where kI is the absorption and $kB(T)$ is the emission. So the fractional absorption in a layer (z, z_1) is

$$\tau(z, z_1) = \exp \left(- \int_{z_1}^z k\rho dz' \right)$$

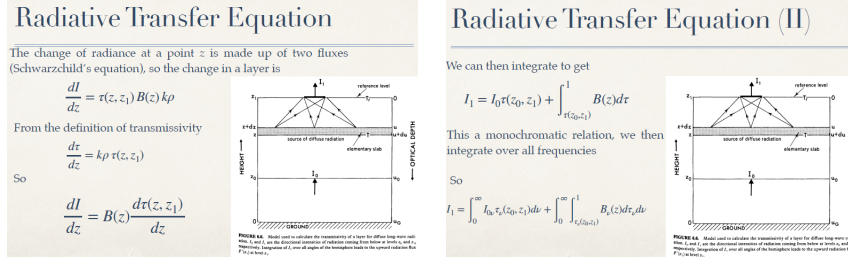


Figure 2.8: Non avevamo voglia di scriverli

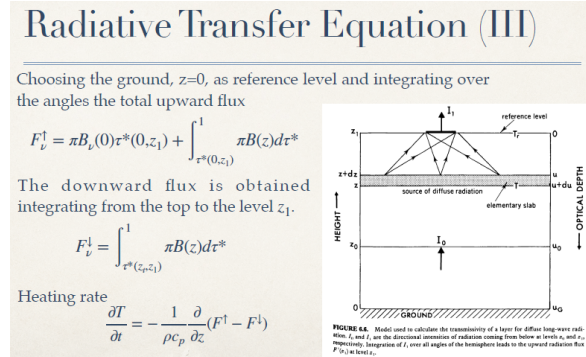


Figure 2.9: Enter Caption

Solar radiation The solar radiation is a function of the zenith angle

$$\cos Z = \sin \varphi \sin \delta + \cos \varphi \cos \delta \cos H$$

where φ is latitude, δ is solar declination, which is the angular distance of the sun north of the equator and varies from about 23.5° on June 22 to -23.5° on December 22 and H is the hour angle, which is the longitudinal distance from the point in question to the meridian of solar noon and therefore is 0 at any point experiencing solar noon. The solar flux, S , entering at the top of the atmosphere is a function of $\cos Z$ and the distance from the sun to the Earth, d , such that

$$S = S_0 f(d) \cos Z$$

where S_0 is the so-called solar constant (the solar energy flux received at the outer atmosphere on a surface normal to the solar beam; known now not to be constant) and the factor $f(d)$ is 1.0344 in early January and 0.9674 in July for the present astronomical conditions. As shown

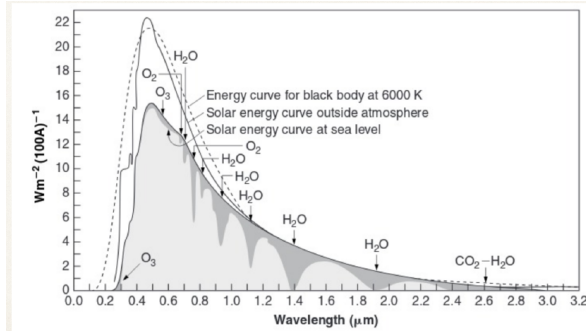


Figure 2.10: Spectral energy distribution as a function of wavelength at the top of the atmosphere and at sea level. The figure includes absorption by various atmospheric gases

in 2.10 the principal absorber in the atmosphere is the stratospheric ozone, which absorbs very effectively in the ultraviolet and in the visible. Water vapor is the primary absorber in the troposphere in the near-infrared, also with carbon dioxide are the main important absorbers for the longer wavelengths.

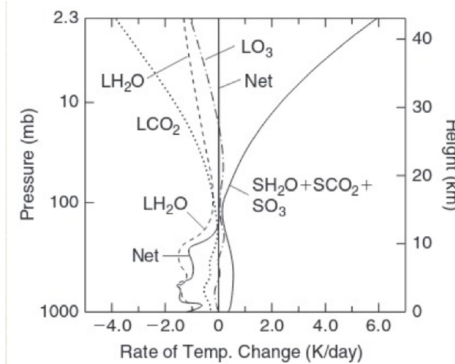


Figure 2.11: Heating rates in the atmosphere due to the absorption of solar radiation by atmospheric gases and due to the longwave or infrared radiation

The largest contributors to the heating/cooling rates are water vapor, carbon dioxide and ozone as shown in Figure 2.11. The net heating/cooling is zero in the stratosphere because in the one-dimensional model, it is in radiative equilibrium. The troposphere shows a net radiative cooling that is compensated by the vertical transfer of sensible and latent heat from below by moist adiabatic convection. As suggested in Figure 2.11 water vapor is the strongest contributor to the troposphere cooling. In the stratosphere cooling due to water vapor, carbon dioxide and ozone is generally compensated by heating due to absorption of solar radiation by zone.

2.6.2 Moisture

In order to discuss precipitation and cloud physics used in climate models, let's introduce basic concepts. *Moisture* is the quantity of water vapor in the air and it can be specified in several ways, depending on which reference is used.

- *mixing ratio* ratio of the density of water vapor to the density of dry air $q = \frac{\rho_w}{\rho}$
- *specific humidity* ratio concerning the density of moist air, the density of water vapor over the total density of the air: $h = \frac{\rho_w}{q_w + \rho}$
- *relative humidity* ratio of the mixing ratio to the saturation mixing ratio $r = \frac{q}{q_s}$

The same as the continuity mass treatment, the changes in the amount of water vapor must be balanced by the moisture sources and sinks

$$\frac{dq}{dt} = \frac{1}{\rho} M + E \quad (2.37)$$

where M is the time rate change of water vapor per unit volume due to condensation or freezing (sinks of moisture) and E is the time rate of change of water vapor content per unit mass due to evaporation from the surface and sub-grid vertical and horizontal diffusion of moisture within the atmosphere (source of moisture). The first term on the right is a sink of moisture, the second is a source of moisture. Often 2.37 is written in flux form by combining with the continuity equation to obtain

$$\frac{\partial(\rho q)}{\partial t} + \nabla \cdot (\rho q \mathbf{V}) + \frac{\partial(\rho q \omega)}{\partial z} = M + \rho E \quad (2.38)$$

If 2.38 is integrated over the entire volume of the atmosphere, the second and the third terms on the left drop out, so that the sources and sinks of moisture must balance to have no secular change in atmospheric moisture over the globe. If the atmosphere is saturated with moisture, then sensible heat can be added to the atmospheric system from latent heat by the conversion of water vapor to liquid warmer or ice parcels.

The first law of thermodynamic must incorporate in the nonadiabatic term, this energy conversion process due to phase changes between liquid, solid, and gas. If the nonadiabatic process of conversion of water vapor to liquid water is the only energy source incorporated, the first law of thermodynamics becomes

$$c_p dT + \frac{1}{\rho} dp = -L dqs$$

The equation of state can be written like

$$e = \rho_W RT$$

where e is the partial pressure for water vapor. Substituting in the previous equation, the mixing ratio becomes now

$$q \approx 0.622 \frac{e}{p} \quad (2.39)$$

Inserting a total differential form of the hydrostatic equation, the first law of thermodynamics becomes

$$\frac{dT}{dz} = -\frac{g}{c_p} - \frac{L}{c_p} \frac{dqs}{dz}$$

taking the log and differentiating the previous equation 2.39 we will obtain

$$\log q_s \approx \log 0.622 + \log e_s - \log p$$

$$\frac{1}{e_s} \frac{de_s}{dz} = \frac{1}{q_s} \frac{dq_s}{dz} + \frac{1}{p} \frac{dp}{dz}$$

$$\frac{1}{e_s} \frac{de_s}{dT} = \frac{1}{q_s} \frac{dq_s}{dz} - \frac{1}{p} g \rho$$

The Clausius-Clapeyron equation relates the change in saturation vapor pressure to the latent heat involved in a phase change from water vapor to liquid water or from liquid water to ice. The most convenient form of this is

$$\frac{1}{e_s} \frac{de_s}{dT} = \frac{L}{RT^2}$$

So we get

$$\frac{dq_s}{dz} = \frac{L q_s}{RWT_2} \frac{dT}{dz} + \frac{g q_s}{RT}$$

$$\Gamma_m = \frac{dT}{dz} = -\frac{g}{c_p} \left(1 + \frac{L q_s}{RT} \right) \left(1 + \frac{L^2 q_s}{c_p RWT_2} \right)^{-1} \quad (2.40)$$

In this way, we will obtain the moist adiabatic lapse rate Γ_m , which is less than the adiabatic lapse rate defined earlier:

$$\Gamma = \frac{dT}{dz} = -\frac{k \rho g}{p} T$$

2.6.3 Clouds

They play a critical role in the radiation characteristics of the Earth's climate, but their radiative properties are not fully understood. In most climate models, the precipitation and convective aspects of the model are used to compute where clouds exist based on whether the atmosphere is near saturation and whether convection is occurring. You can use different parameters to explain that.

Cumulus formation

If a parcel of air near the Earth's surface (at an atmospheric pressure of approximately 1000 mb) starts to rise, say from strong heating, it will cool at approximately the dry adiabatic lapse rate of 9.8 K km^{-1} . When the parcel cools sufficiently the parcel is saturated, gaining a condition of instability because there is much more energy in the water vapor. The level at which this occurs is termed the lifting condensation level, LCL, and is typically at the cloud base as the picture below shows. If the parcel does not rise high enough to reach an LCL, then a cloud should not form. From the LCL upward, the parcel will cool less rapidly as it rises since the latent heat of condensation or fusion releases heat. This lessened rate of temperature decrease with height is the moist adiabatic lapse rate.

As shown in figure 2.13 the dotted curve represents conditions for the environmental air, and the solid curves represent conditions for the path along which a parcel will ascend from point A to B, depending on whether the dry or the moist adiabatic lapse rate is appropriate. There is a point B' highlighted on the curve for the environmental air that is colder in both cases than point B for the parcel at the same height. Since the air at B' is colder than that at B, the parcel will have positive buoyancy. Thus in principle, it will continue ascending. If on the other hand, a parcel is at C and ascends to point D, it will be colder than the surrounding environmental air at D'. Thus the parcel will have negative buoyancy, which will cause it to sink to its original position.

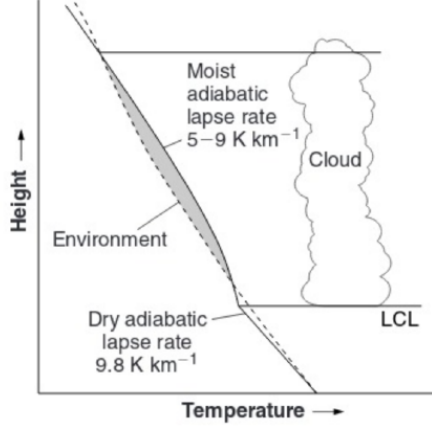


Figure 2.12: Enter Caption

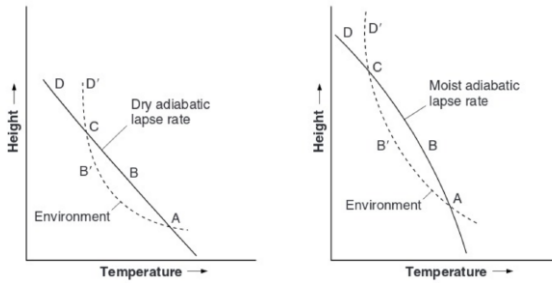


Figure 2.13: Diagram of stable and unstable conditions concerning dry and moist lapse rates.

2.6.4 Surface Processes

Boundary fluxes for momentum and heat, we can physically represent as

$$\tau_x = \rho C_D |\mathbf{v} - \mathbf{v}_s| (u_s - u)$$

$$\tau_y = \rho C_D |\mathbf{v} - \mathbf{v}_s| (v_s - v)$$

$$H = \rho c_p C_H |\mathbf{v} - \mathbf{v}_s| (\theta_s - \theta)$$

$$LE = \rho L_C E |\mathbf{v} - \mathbf{v}_s| (q_s - q)$$

Where over land \mathbf{v} is zero.

Above the surface boundary layer adjacent to Earth's surface exists the planetary boundary layer, where the wind turns with the height. Within this region, the balance of forces can be approximated by Coriolis, pressure gradient, and frictional forces through the following simplification

$$-f_\nu = -\frac{1}{\rho a \cos \varphi} \frac{\partial p}{\partial \lambda} + F_\lambda$$

$$f_u = -\frac{1}{\rho a} \frac{\partial p}{\partial \varphi} + F_\varphi$$

The frictional term can be expressed as the vertical gradient of stress, so that

$$F_\lambda = \frac{1}{\rho} \frac{\partial \tau_\lambda}{\partial z}$$

and

$$F_\varphi = \frac{1}{\rho} \frac{\partial \tau_\varphi}{\partial z}$$

and the stress can in turn be related to the vertical gradient of wind shear

$$\tau_\lambda = \rho K_m \frac{\partial u}{\partial z}$$

and

$$\tau_\varphi = \rho K_m \frac{\partial v}{\partial z}$$

where K_m is the vertical eddy or transfer coefficient for momentum. Note that if the vertical wind shear is large, as one would expect near the Earth's surface since the wind must approach zero at the surface, then the momentum transfer is also large. On the molecular scale, K_m , takes on values appropriate for those space scales; however, in the atmosphere and ocean models the space scales are much larger. Many of the eddies have dimensions of the order of the spatial grid structure of the models. If the layer is unstable there is strong vertical mixing and K_m is large; if the layer is stable there is no strong coupling and K_m is small. A useful measure of this stability is the Richardson number R_i , which is defined as

$$R_i = \frac{g}{\theta} \frac{\frac{\partial \theta}{\partial z}}{\left(\frac{\partial V}{\partial z}\right)^2}$$

where $V = |\mathbf{V}|$ and $\frac{\partial V}{\partial z}$ is the vertical wind shear or vertical gradient of wind velocity.

2.6.5 Hydrology

$$\frac{\partial \zeta}{\partial t} = - \nabla \cdot (\zeta + f) \vec{V}$$

$$\frac{\partial \zeta}{\partial t} = - (\zeta + f) \nabla \cdot \vec{V} - \vec{V} \cdot \nabla (\zeta + f)$$

$$\frac{\partial \zeta}{\partial t} = - (\zeta + f) D - \vec{V} \cdot \nabla (\zeta + f)$$

Figure 2.14: Schematic processes and features relevant to surface hydrology and evapotranspiration

As shown in 2.14 lots of processes are involved in surface hydrology. These include radiation, sensible heat, evaporation, transpiration, momentum, and precipitation, but also H₂O and CO₂ fluxes. The surface moisture can contribute to surface flow in streams percolate to a deeper layer or even become groundwater, depending on the porous properties of the ground. In the root zones of plants, some of the surface moisture can be taken up by the plant roots and then relayed to the plant leaves and transpired.

Within a land area as large as a horizontal grid cell of a global model, there are generally multiple surface types, including lakes, wetlands, different vegetation types, and different soil types. Another aspect of land surface processes being improved in many climate models is the simulation of snow coverage. The snow modeling community has developed a variety of models that can be used for climate and hydrology. These models range from the simple to the complex, and several of them are specifically designed for use in general circulation models. The more complex snow models take into account melting processes, grain size, shape, liquid water content, and percolation processes.

Appendix A

Mathematical Complements

Last updated: 2024-12-09

Source file: [appendixA.tex](#)

A.1 Vector calculus

A.1.1 Gradient

The gradient measures the rate and direction of the steepest increase of a scalar field. It is a vector operation applied to a scalar field, and the result is a vector field. Mathematically, for a scalar field $\psi(x, y, z)$ the gradient is defined as (in cartesian coordinates):

$$\nabla\psi = \left(\frac{\partial\psi}{\partial x}, \frac{\partial\psi}{\partial y}, \frac{\partial\psi}{\partial z} \right) \quad (\text{A.1})$$

The gradient points in the direction where the scalar field f increases most rapidly. The magnitude of the gradient gives the rate of increase in that direction. In thermodynamics, the gradient of temperature describes the direction and rate of heat flow. The result of a gradient is a vector.

The gradient operator in the usual earth spherical coordinate system described in Section 2.1.1 reads

$$\nabla\psi = \frac{1}{r}\frac{\partial\psi}{\partial\phi}\hat{\mathbf{e}}_\phi + \frac{1}{r\cos\phi}\frac{\partial\psi}{\partial\lambda}\hat{\mathbf{e}}_\lambda + \frac{\partial\psi}{\partial z}\hat{\mathbf{k}} \quad (\text{A.2})$$

A.1.2 Divergence

In vector calculus, divergence measures the rate at which a vector field spreads out or converges at a given point. It quantifies how much the field “diverges” from or “converges” into a region. For a **vector field** $\psi = (\psi_x, \psi_y, \psi_z)$ the divergence is defined as (in cartesian coordinates):

$$\nabla \cdot \psi = \frac{\partial\psi_x}{\partial x} + \frac{\partial\psi_y}{\partial y} + \frac{\partial\psi_z}{\partial z}. \quad (\text{A.3})$$

In the usual earth spherical coordinates system of Section 2.1.1, Equation A.3 for a vector field $\psi = (\psi_\phi, \psi_\lambda, \psi_z)$ reads

$$\nabla \cdot \psi = \frac{1}{r}\frac{\partial\psi_\lambda}{\partial\lambda} + \frac{1}{r\cos\phi}\frac{\partial\psi_\phi}{\partial\phi} + \frac{\partial\psi_z}{\partial z}. \quad (\text{A.4})$$

A positive divergence, i.e. $\nabla \cdot \psi > 0$, indicates a field that is “spreading out” or “expanding” at a point. An example might be that of a source emitting fluid, such as water spraying out of a fountain. On the other hand $\nabla \cdot \psi < 0$ means the field is “converging” or “contracting” at a point. For instance, take a sink where fluid flows inward, such as water draining into a hole. Finally, $\nabla \cdot \psi = 0$ describes a field that is neither expanding nor contracting, often indicating an incompressible flow. An example is a steady incompressible flow of a fluid.

A.1.3 Curl

The curl of a vector field measures the tendency of the field to induce rotation around a point, or how much the field “circulates” locally. It is a vector operation applied to a vector field, and the result is another vector field. For a **vector field** $\psi = (\psi_x, \psi_y, \psi_z)$ the curl is defined as (in cartesian coordinates):

$$\nabla \times \psi = \begin{vmatrix} \hat{\mathbf{i}} & \hat{\mathbf{j}} & \hat{\mathbf{k}} \\ \frac{\partial}{\partial x} & \frac{\partial}{\partial y} & \frac{\partial}{\partial z} \\ \psi_x & \psi_y & \psi_z \end{vmatrix} \quad (\text{A.5})$$

In the usual earth spherical coordinates system of Section 2.1.1, Equation A.5 for a vector field $\psi = (\psi_\phi, \psi_\lambda, \psi_z)$ reads

$$\nabla \times \psi = \frac{1}{r \cos \phi} \begin{vmatrix} \hat{\mathbf{e}}_\phi & r \cos \phi \hat{\mathbf{e}}_\lambda & \hat{\mathbf{k}} \\ \frac{\partial}{\partial \phi} & \frac{\partial}{\partial \lambda} & \frac{\partial}{\partial z} \\ \psi_\phi & r \cos \phi \psi_\lambda & \psi_z \end{vmatrix} \quad (\text{A.6})$$

Expanding Equation A.6 gives:

$$\nabla \times \psi = \hat{\mathbf{k}} \frac{1}{r \cos \phi} \left[\frac{\partial \psi_\phi}{\partial \lambda} - \frac{\partial}{\partial \phi}(\psi_\lambda \cos \phi) \right] + \hat{\mathbf{e}}_\phi \frac{1}{r} \left(\frac{\partial \psi_z}{\partial \lambda} - \frac{\partial \psi_\lambda}{\partial z} \right) + \hat{\mathbf{e}}_\lambda \frac{1}{r} \left(\frac{\partial \psi_\phi}{\partial z} - \frac{\partial \psi_z}{\partial \phi} \right) \quad (\text{A.7})$$

The curl outputs a vector field whose direction indicates the axis of rotation (using the right-hand rule), and whose magnitude indicates the strength of the rotation. The curl represents the amount and direction of rotational motion or “swirl” in the field. In fluid dynamics, a region of nonzero curl corresponds to vorticity, where fluid particles rotate.

A.2 Spherical harmonics

Spherical harmonics are key mathematical functions in the expansion of scalar and vector fields on the surface of a sphere. In climate modeling, they are extensively used for representing atmospheric and oceanic variables, such as temperature, pressure, and wind patterns, on the spherical surface of Earth.

Let’s break down the **spherical harmonics expansion** in more detail, looking at its mathematical formulation, properties, and applications, especially in the context of climate modeling.

A.2.1 Mathematical Definition of Spherical Harmonics

The spherical harmonics $Y_l^m(\theta, \phi)$ are solutions to the Laplace equation on the sphere. They depend on two angular coordinates, **latitude** (θ) and **longitude** (ϕ). The general form of a spherical harmonic is:

$$Y_l^m(\theta, \phi) = N_l^m P_l^m(\cos \theta) e^{im\phi}$$

Where:

- l is the **degree** of the harmonic, a non-negative integer ($l = 0, 1, 2, 3, \dots$).
- m is the **order** of the harmonic, an integer satisfying $-l \leq m \leq l$
- $P_l^m(\cos \theta)$ are the **associated Legendre polynomials**, which define the angular part of the function in terms of the **colatitude** (θ).
- $e^{im\phi}$ is a complex exponential that encodes the **longitudinal** dependence, where m controls the azimuthal symmetry.

Normalization Constant: The spherical harmonics are typically normalized such that:

$$N_l^m = \sqrt{\frac{(2l+1)(l-|m|)!}{4\pi(l+|m|)!}}$$

This ensures that the spherical harmonics are **orthonormal** over the surface of the sphere. That is:

$$\int_0^\pi \int_0^{2\pi} Y_l^m(\theta, \phi) \overline{Y_{l'}^{m'}(\theta, \phi)} \sin \theta d\theta d\phi = \delta_{l,l'} \delta_{m,m'}$$

where $\overline{Y_l^m}$ is the complex conjugate of Y_l^m , and δ is the **Kronecker delta**, which equals 1 if the indices are equal, and 0 otherwise.

A.2.2 Spherical Harmonics Expansion of Functions on the Sphere

Given a scalar field $f(\theta, \phi)$ defined on the surface of a sphere (such as the Earth's atmosphere), we can expand it in terms of spherical harmonics as a series:

$$f(\theta, \phi) = \sum_{l=0}^L \sum_{m=-l}^l a_l^m Y_l^m(\theta, \phi)$$

Here:

- L is the **truncation level**, which determines the maximum degree of spherical harmonics included in the expansion.
- a_l^m are the **spectral coefficients** that need to be determined.

Computing the Coefficients: To find the spectral coefficients, we use the orthonormality of the spherical harmonics. The coefficient a_l^m is given by the integral:

$$a_l^m = \int_0^\pi \int_0^{2\pi} f(\theta, \phi) \overline{Y_l^m(\theta, \phi)} \sin \theta d\theta d\phi$$

This integral projects the function $f(\theta, \phi)$ onto the spherical harmonic $Y_l^m(\theta, \phi)$, extracting the corresponding coefficient.

Truncation of the Series: In practice, we do not include all spherical harmonics. Instead, we truncate the sum at some maximum value of $l=L$, which results in a finite series expansion. The truncation determines the **spectral resolution** of the model and defines the number of spherical harmonic modes included in the representation of the field.

For example:

- If $L = 10$, then the expansion includes all spherical harmonics from degree $l = 0$ up to $l = 10$.
- The total number of terms in the expansion is given by the sum $\sum_{l=0}^L (2l+1)$, which grows roughly as L^2 .

For $L = 10$, the total number of terms is:

$$N_{terms} = \sum_{l=0}^{10} (2l+1) = 1 + 3 + 5 + 7 + 9 + 11 + 13 + 15 + 17 + 19 + 21 = 100$$

so, the function $f(\theta, \phi)$, is approximated by a sum of 100 spherical harmonic terms.

A.2.3 Properties of Spherical Harmonics

Orthogonality and Completeness: Spherical harmonics are **orthogonal** over the surface of the sphere, meaning that any two different harmonics Y_l^m and $Y_{l'}^{m'}$ are perpendicular in the function space. This property makes them ideal for decomposing a function into distinct components.

Additionally, the set of spherical harmonics forms a **complete basis** for any square-integrable function defined on the sphere. This means that any smooth function $f(\theta, \phi)$ can be represented as a (potentially infinite) sum of spherical harmonics.

Symmetry:

- The degree l of a spherical harmonic determines the **angular scale** of the feature. Large values of l correspond to smaller-scale features (higher-frequency components), while small values of l correspond to large-scale, low-frequency components.
- The order m determines the **longitudinal symmetry**. For each l there are $2l + 1$ distinct values of m ranging from $-l$ to l corresponding to different symmetries of the field in the longitudinal direction.

For example:

- The spherical harmonic $Y_1^0(\theta, \phi)$ corresponds to a dipole, with a variation in latitude but no longitudinal variation.
- The spherical harmonic $Y_2^1(\theta, \phi)$ corresponds to a pattern with more complex longitudinal symmetry.

Scaling: The spherical harmonics have a natural scaling property. For instance, multiplying a spherical harmonic by a constant factor will change the amplitude of the corresponding mode without affecting the symmetry of the function. This property is useful for scaling fields, such as wind speeds or temperature distributions, in climate models.

A.2.4 Applications of Spherical Harmonics in Climate Models

In climate and weather models, spherical harmonics are used to represent global fields with high accuracy and relatively few coefficients, which is especially useful for simulating large-scale atmospheric dynamics.

Some specific applications include:

Atmospheric Dynamics:

- Atmospheric models often represent variables like pressure, temperature, and wind in terms of spherical harmonics. By expanding these fields in spherical harmonics, models can capture large-scale features such as the **zonal wind**, **jet streams**, and **planetary waves** with fewer coefficients than would be required for grid-based methods.
- For example, the **vorticity equation** or the **primitive equations** of motion are often solved in spectral space, and spherical harmonics are used to expand the relevant fields.

Global Climate Models (GCMs):

- In GCMs, the Earth's climate is simulated by solving for variables (e.g., temperature, pressure, wind) at each point on the sphere. By using spherical harmonics, GCMs can efficiently model the global climate while avoiding the need for very fine grids (which would be computationally expensive).
- **Spectral Finite-Difference Models:** Some models combine the benefits of spectral methods for large-scale patterns with finite-difference methods for localized phenomena (like convection or boundary layers), allowing for efficient simulations of both large-scale and small-scale processes.

Ocean Models: Similar to atmospheric models, ocean circulation models may use spherical harmonics to represent the spatial structure of the ocean's surface currents, sea level anomalies, and other global patterns.

Data Assimilation: In data assimilation methods, spherical harmonics can be used to represent the state of the atmosphere or ocean at a given time, with spectral coefficients used to update the model's state based on observations.

A.3 EOF: Empirical Orthogonal Functions

Definition A.3.1: EOF

The Empirical Orthogonal^a Functions methods is a for analyzing large datasets that vary over both space and time; it helps to extract dominant patterns of variability in a data set.

^a*empirical*= derived from data, *orthogonal*= the scalar product is zero.

How does it work?

1. Matrix representing spatiotemporal data $\mathbf{X}(i, j)$:
rows $i \rightarrow$ time steps
columns $j \rightarrow$ spatial points
2. To identify the major patterns of variability we compute the covariance matrix of the data. It describes how each spatial location's data varies in relation to every other location:

$$\mathbf{C} = \text{COV} = \frac{1}{n} \mathbf{X}^T \mathbf{X}$$

where $\mathbf{X} = \mathbf{X}(i, j) - \bar{\mathbf{X}}_j$

3. The covariance matrix is decomposed into eigenvalues and eigenvectors \rightarrow SINGULAR VALUE DECOMPOSITION SVD:

$$\mathbf{Cv} = \lambda v$$

with v eigenvector or spatial patterns, λ eigenvalues (it describes the variance expressed by each pattern). In this way we get how each data location relates to others.

4. Projecting the original data into these v we obtain the PRINCIPAL COMPONENTS that show how each spatial pattern evolves over time.

$$\text{PC}(t) = \mathbf{X} \cdot v$$

Therefore,

- EOFs (=eigenvectors) represent the dominant spatial patterns in data, each shows a specific pattern variability over space (e.g. how T pattern shifts across the globe).
- PCs (principal components) are the time series corresponding to each EOF.

The eigenvalues tell how much variance each EOF captures: if they capture most of the variance it means they represent the major patterns in the data. EOF and PCs (Principal Component Analysis) are the same techniques mathematically but the EOF goal is to find SPATIAL PATTERNS and their corresponding TIME EVOLUTION; while the PCA aims to find the directions of maximum variance in data irrespective of space and time. PCA helps in dimensionality reduction.

Note. The diagonal I find after the eigenvalue decomposition is the sum of the covariants:

$$\mathbf{X} = \mathbf{U}\Sigma\mathbf{V}^T \quad \text{so that} \quad \mathbf{S} = \mathbf{X}\mathbf{X}^T = \mathbf{U}\Sigma^2\mathbf{U}^T$$

In \mathbf{U} are the eigenfunctions associated to the covariant, in Σ the eigenvalues.

When you have a time serie of data, you should organize them in some order: a matrix where every row ($1 \leq j \leq n$) is a time variation, hence every vector is a space variation of some place in the same tame:

$$\mathbf{X} = [\mathbf{X}_1, \mathbf{X}_2, \dots, \mathbf{X}_n]$$

$$\mathbf{S} = \frac{1}{1-n} \mathbf{X}\mathbf{X}^T$$

on the diagonal of \mathbf{S} , you have the same location (covariance relation), every other element is the covariance of two different locations (it defines how two locations are connected in time):

$$\text{Tr}(\mathbf{S}) = \sum \sigma^2$$

. It becomes a correlation matrix if divided by the standard deviations of the locations. $\mathbf{X}\mathbf{X}^T$ as symmetric, meaning the eigenvalues are positive and eigenvectors are orthogonal. The eigenvectors represent the EOF. The single value decomposition tells us that any matrix can be written in terms of 2 different other orthogonal matrices: $\mathbf{X} = U\Sigma V^T$. I could simply take the data matrix and compute the SVD:

$$x(i) = \sum_i \mathbf{u}_i \sigma_i v_i$$

how much covariance the pattern u of EOF corresponding to the singular value decomposition is responsible for:

$$\mu_i = \frac{\sigma_i^2}{\sum_{i=1}^n \sigma_i^2}$$

A.3.1 Eigenvalue decomposition → Singular Value Decomposition

It helps to understand what is the weight of the \mathbf{u}_i component in the \mathbf{x} dataset.

orthogonal matrix $\mathbf{U}\mathbf{U}^T = \mathbf{I} \rightarrow$ they are rotating operating on one vector. You could take any transformation breaking it into 3 processes:

rotation → stretching (diagonal matrix) → rotation

If I can decompose $\mathbf{S} = \mathbf{U}\Sigma^2\mathbf{U}^T$. Note that the $\text{tr}(\Sigma) = \mathbf{S}$. The number of columns in $\mathbf{U} = \Sigma_{ij}$ where t_i is the number of time variations and x_j the number of features.

Every column in the data matrix can be expanded:

$$\mathbf{x}(t) = \sum_i \mathbf{u}_i \sigma_i v_i(t)$$

with u_i = patterns, σ_i = singular value and v_i weight of the pattern i at that particular time. $\mathbf{x} = \mathbf{u}_i$ in terms of vector with the same length. EOF method defines only the independent variables.

SST (lat,long) \rightarrow transforms into a vector $\rightarrow \begin{bmatrix} \text{lat}_1 \\ \text{lat}_2 \\ \dots \\ \text{lat}_n \end{bmatrix} \rightarrow$ I can represent them in a map. (u_i and v_i compensate each other).

Higher EOF means more zero lines, meaning more oscillations.

A.3.2 Limitations

- because of the + and - we are imposing a structure looking for patterns that are orthogonal (we exclude data)
- thinking of EOF as oscillations

A.3.3 Variance

The variance of the data \mathbf{X} is defined as

$$\sigma^2 = \sum_{i=1}^n \frac{(x_i - \bar{x})^2}{n} \quad (\text{A.8})$$

A.3.4 Covariance

Basically it is a straight multiplication. It's a statistical measure that indicates the degree to which two random variables change together. If two variables tend to increase or decrease in tandem then $\text{COV} > 0$; if one tends to increase while the other decreases, then $\text{COV} < 0$.

$$\text{COV}(\mathbf{X}, \mathbf{Y}) = \frac{1}{n} \sum_{i=1}^n (x_i - \bar{x})(y_i - \bar{y}) \quad (\text{A.9})$$

Covariance helps identify the relationship between two variables but it does not provide information about the strength or scale of the relationship \rightarrow correlation.

A.3.5 Correlation

Statistical measure that describes the strength and direction of a linear relationship between two variables. It STANDARDIZES the relationship, providing a dimensionless value that ranges between -1 and 1 .

$$r = \frac{\text{COV}(\mathbf{X}, \mathbf{Y})}{\sigma_x \sigma_y} \quad (\text{A.10})$$

σ_i are the standard deviations.

- $r = 1$ perfect positive linear relation
- $r = -1$ perfect negative linear relation
- $r = 0$ no linear relation

A.4 Space-time splittings

The dominant shape of the global circulation suggests that some understanding can be gained from splitting the physical fields into larger and smaller portions using appropriate averages. At a first inspection, the flow is seen as a predominant circumpolar vortex with superposed fluctuations in space and time. The longitudinal direction is also known as the “zonal” direction, therefore the average over longitude is known as the zonal averaging

A.4.1 Zonal means

The zonal mean of a quantity A is defined as the average over longitudes. Commonly used symbols in the literature are the overbar \bar{u} or square brackets $[u]$, the first is most frequently encountered in the theoretical and modeling literature whereas the second is most commonly used in observational and diagnostics works. In the following, we will denote the zonal mean of a field A as:

$$[A] = \frac{1}{2\pi} \int_0^{2\pi} A dx \quad (\text{A.11})$$

so that the entire field can be decomposed into

$$A = [A] + A^* \quad (\text{A.12})$$

where A^* is the deviation from the zonal mean. The average has the properties that $[[A]] = [A]$ and $[A^*] = 0$.

When a stream function can be defined, the average zonal mean meridional velocity is zero:

$$[v] = \frac{1}{2\pi} \int_0^{2\pi} v dx = \frac{1}{2\pi} \int_0^{2\pi} \frac{\partial \psi}{\partial x} dx = 0 \quad (\text{A.13})$$

This is a consequence of the more general result that the zonal mean of any quantity that is a longitude derivative is zero.

A.4.2 Time means

The time mean is defined simply as the average over a length of time. As for the zonal mean (Equation A.11), multiple symbols are employed. Here we denote the time mean of a field A with:

$$\bar{A} = \frac{1}{T} \int_0^T A dt \quad (\text{A.14})$$

so that the total field is

$$A = \bar{A} + A' \quad (\text{A.15})$$

The deviations from the zonal means are called “eddy” components. An eddy that obeys a dispersion relation is a “wave”.

A.4.3 Higher order quantities

The averages can be used to decompose higher-order quantities. For instance using zonal means a quadratic correlation of the form AB can be decomposed as

$$AB = ([A] + A^*)([B] + B^*) = A^*B^* + [A]B^* + A^*[B] + [A][B] \quad (\text{A.16})$$

If we take the zonal mean of Equation A.16, i.e. the second order mean of AB , we end up with the following decomposition:

$$[AB] = [A^*B^* + [A]B^* + A^*[B] + [A][B]] = [A][B] + [A^*B^*] \quad (\text{A.17})$$

where the mix terms disappear as $[A^*] = 0$.

We can refine the splitting by considering the time average splitting of the zonal terms:

$$= \overline{[A]} + [A]' A^* = \overline{A}^* + A'^* \quad (\text{A.18})$$

These terms represent the stationary symmetric circulation, the transient symmetric circulation and the stationary deviation from the zonal means (“asymmetries”) and the transient asymmetries. Inserting these relations into Eq. A.17 we get

$$= (\overline{[A]} + [A]')(\overline{[B]} + [B]') + [A^* B^*] \quad (\text{A.19})$$

the time mean of the terms linear in the time deviation will average again to zero (this time with respect the time mean) and we finally get

$$\overline{[AB]} = \overline{[A][B]} + \overline{[A]'[B]'} + \overline{[A^* B^*]} \quad (\text{A.20})$$

The decompositions are not unique. We have first performed the split in the zonal mean and then the split in the time mean, considering a split only in the eddy part:

$$A^* = \overline{A}^* + A'^* \quad (\text{A.21})$$

we would get

$$\overline{[AB]} = \overline{[A][B]} + \overline{[\overline{A}^* \overline{B}^*]} + \overline{[A'^* B'^*]} \quad (\text{A.22})$$

where the first term is the contribution of the mean meridional circulation, the second is the contribution of the time-mean (standing) eddies and the last one is the contribution of the transient eddies. This kind of decomposition is therefore a useful instrument but requires always consideration of the hypothesis formulated in the initial design. Another consideration is that they depend on the specific kind of averaging that is used. There is little choice in the zonal mean, being fixed by the geometry, but we have much more choices in the case of the time mean. Results will depend on the length of the time averaging period and on the original frequency of the data. Time mean and second-order quantities calculated over daily will differ from the same quantities calculated over time series of weekly or monthly data. There is no *correct* choice, each one will offer a different glimpse in the data from a chosen perspective.

Bibliography

- Dobson, G. M. B. (1968). *Exploring the Atmosphere*. Oxford: Clarendon Press. 209 pp.
- Gill, Adrian E. (1982). *Atmosphere-Ocean Dynamics*. Vol. 30. International Geophysics Series. Orlando, FL, USA: Academic Press. 662 pp.
- Trenberth, Kevin E. and John T. Fasullo (July 1, 2012). “Tracking Earth’s Energy: From El Niño to Global Warming”. In: *Surveys in Geophysics* 33.3, pp. 413–426.
- Washington, W. and C. Parkinson (2005). *An Introduction to Three-Dimensional Climate Modeling*. 2nd Edition. University Science Books. 380 pp.
- Zanotti, Niccolò (Dec. 2023). “Rheology-Based Sea Ice Dynamics: From the Fluid-like to the State-of-the-Art Solid-like Brittle Approach.” In: *University of Bologna Institutional Theses repository*.

